Control of mRNA Stability in Fungi by NMD, EJC and CBC Factors Through 3′UTR Introns

Ying Zhang and Matthew S. Sachs[1]
Department of Biology, Texas A&M University, College Station, Texas 77843-3258
ORCID IDs: 0000-0002-1238-0456 (Y.Z.); 0000-0001-9891-9223 (M.S.S.)

ABSTRACT In higher eukaryotes the accelerated degradation of mRNAs harboring premature termination codons is controlled by nonsense-mediated mRNA decay (NMD), exon junction complex (EJC), and nuclear cap-binding complex (CBC) factors, but the mechanistic basis for this quality-control system and the specific roles of the individual factors remain unclear. Using *Neurospora crassa* as a model system, we analyzed the mechanisms by which NMD is induced by spliced 3′-UTR introns or upstream open reading frames and observed that the former requires NMD, EJC, and CBC factors whereas the latter requires only the NMD factors. The transcripts for EJC components eIF4A3 and Y14, and translation termination factor eRF1, contain spliced 3′-UTR introns and each was stabilized in NMD, EJC, and CBC mutants. Reporter mRNAs containing spliced 3′-UTR introns, but not matched intronless controls, were stabilized in these mutants and were enriched in mRNPs immunopurified from wild-type cells with antibody directed against human Y14, demonstrating a direct role for spliced 3′-UTR introns in triggering EJC-mediated NMD. These results demonstrate conclusively that NMD, EJC, and CBC factors have essential roles in controlling mRNA stability and that, based on differential requirements for these factors, there are branched mechanisms for NMD. They demonstrate for the first time autoregulatory control of expression at the level of mRNA stability through the EJC/CBC branch of NMD for EJC core components, eIF4A3 and Y14, and for eRF1, which recognizes termination codons. Finally, these results show that EJC-mediated NMD occurs in fungi and thus is an evolutionarily conserved quality-control mechanism.

KEYWORDS nonsense-mediated mRNA decay (NMD); RNA stability; exon junction complex (EJC); cap-binding complex (CBC); spliced 3′-UTR intron; post-transcriptional control; ribosome; translation; *Neurospora crassa*

THE nonsense-mediated mRNA decay (NMD) pathway targets mRNA for degradation through the recognition of translated termination codons determined to be premature (Nicholson *et al.* 2009; Kervestin and Jacobson 2012; Popp and Maquat 2013). The NMD pathway can degrade mRNAs that contain upstream open reading frames (uORFs) or long 3′-UTRs. The termination-related processes that trigger uORF-mediated or long 3′-UTR-mediated NMD are considered to be similar (Amrani *et al.* 2004, 2006; Nicholson *et al.* 2009) in that termination events occurring far from the context created by the mRNA poly(A) tail can result in mRNA degradation (the "faux-UTR" model). In higher eukaryotes, NMD can also act on mRNAs that contain an intron downstream of a termination codon, such as aberrantly spliced transcripts or 3′-UTR intron-containing transcripts (Sauliere *et al.* 2010; Bicknell *et al.* 2012). When a spliced intron is positioned at least 50–55 nt downstream of a termination codon, the exon junction complex (EJC) positioned near the exon–exon junction is not displaced by translating ribosomes and its continued association with mRNA targets the mRNA for degradation by NMD (Isken and Maquat 2007). While there are some shared factors, such as the UPF factors, this branch of NMD appears distinct from the faux-UTR branch in that, for NMD to occur, it requires an EJC to remain on the mRNA downstream from the termination event that triggers NMD.

In mammals, the nuclear cap-binding complex (CBC), which is composed of CBP80 and CBP20, is preferentially associated with mRNAs undergoing EJC-targeted NMD (Ishigaki *et al.* 2001). This has led to a model in which EJC-mediated targeting of mRNAs for NMD occurs during pioneer rounds of translation. During these pioneer rounds, CBC has not yet been replaced by eIF4E, the cytoplasmic cap-binding protein (Maquat *et al.* 2010). The implication

doi: 10.1534/genetics.115.176743
Manuscript received March 25, 2015; accepted for publication June 1, 2015; published Early Online June 4, 2015.
Supporting information is available online at http://www.genetics.org/lookup/suppl/doi:10.1534/genetics.115.176743/-/DC1.
[1]Corresponding author: Department of Biology, Texas A&M University, College Station, TX 77843-3258. E-mail: msachs@bio.tamu.edu

of these studies was that the CBC must also be associated with the mRNA for EJC-mediated NMD to occur. However, more recent data show that EJC-mediated NMD can occur on mRNAs associated with the cytoplasmic cap-binding factor eIF4E (Durand and Lykke-Andersen 2013; Rufener and Muhlemann 2013; Popp and Maquat 2014), and the role of the CBC in NMD, and even whether it is essential for this process (Hosoda *et al.* 2005; Dzikiewicz-Krawczyk *et al.* 2008), is not fully understood.

EJC-mediated NMD has been observed in animals and plants, but in the budding yeast *Saccharomyces cerevisiae*, multiple components of the EJC, and EJC-mediated NMD, are lacking, and in fission yeast *Schizosaccharomyces pombe*, while EJC components are present, a role for them in determining mRNA stability via NMD-related pathways has not been demonstrated (Wen and Brogna 2010). Thus a comprehensive understanding of the evolutionary significance of EJC and CBC factors in NMD and the means to dissect the functions of the EJC and CBC factors that contribute to NMD in highly tractable model fungal systems remain lacking.

The filamentous fungi generally encode NMD and EJC machinery (Feldbrugge *et al.* 2008). In *Aspergillus nidulans*, a role for *nmdA*, the *upf2* homolog, has been identified in the control of mRNA stability (Morozov *et al.* 2006) and the recognition of premature stop codons through *upf1* is associated with additional processes affecting mRNA degradation (Morozov *et al.* 2012). The genome of the model filamentous fungus *Neurospora crassa* contains homologs of the NMD components UPF1, UPF2, and UPF3, the core EJC components eIF4A3, Mago, and Y14, and CBC components CBP20 and CBP80. A role for *upf1* in *N. crassa* biology is indicated by identification of alleles causing a circadian rhythm defect (Compton 2003). The molecular basis for this circadian defect—a short period—is not known.

Measurement of mRNA stability is critical for determining whether NMD, EJC, or CBC mutations directly or indirectly affect mRNA levels. Metabolic labeling with 4-thiouracil (4TU) can be used to examine mRNA half-life (Cleary *et al.* 2005). We developed methods for using metabolic labeling of mRNA with 4TU in pulse–chase analyses to measure mRNA stability in *N. crassa*. We used this approach to examine the effects of deletions of *N. crassa* genes specifying NMD, EJC, and CBC factors on the stability of endogenous mRNAs and reporter mRNAs that contain uORFs or 3′-UTR introns. These data show that *N. crassa* NMD factors can control the stability of mRNAs containing uORFs or spliced 3′-UTR introns and that *N. crassa* NMD, EJC, and CBC factors can control the stability of mRNAs containing 3′-UTR introns. These data show for the first time that the CBC is essential for NMD of mRNAs induced by spliced introns downstream from termination codons. Importantly, mRNAs demonstrated to be under EJC/CBC control include those encoding the EJC components eIF4A3 and Y14, and the translation termination factor eRF1, indicating that the RNA decay pathways in which these factors are involved have roles in determining cellular levels of these factors through autoregulation of their mRNA levels. These results provide new insight into the mechanistic basis of NMD in eukaryotes and demonstrate for the first time that major branches of NMD are conserved between higher eukaryotes and fungi.

Materials and Methods

Strains

N. crassa strains obtained from the Fungal Genetics Stock Center (FGSC) (McCluskey *et al.* 2010) included FGSC11230 (ΔNCU04242, *Δupf1)*, FGSC15706 (ΔNCU05267, *Δupf2)*, FGSC11679 (ΔNCU03435, *Δupf3)*, FGSC15492 (ΔNCU03226, *Δy14)*, FGSC13031 (ΔNCU04405, *Δmago)*, FGSC19228 (ΔNCU06678, *Δxrn1)*, FGSC18692 (ΔNCU00210, *Δcpb20)*, FGSC22440 (ΔNCU04187, *Δcpb80)*, FGSC16561 (ΔNCU01446, *Δuc-4)*, and the wild- type (wt) sequenced strain FGSC 2489 (74-OR23-1V A). The deletion mutants were produced by the functional genomics program (Colot *et al.* 2006).

Homokaryotic isolates with desired genotypes were obtained by selecting appropriate progeny from sexual crosses (Davis and de Serres 1970) or by selecting appropriate culture isolates following purification of asexually produced uninucleate microconidia (Ebbole and Sachs 1990). Purification by microconidiation was performed as described except that microconidia were pelleted in an Eppendorf 5415D centrifuged at 12000 × *g* for 2 min and, following resuspension and plating, germinated at 30°. Homokaryons were confirmed by PCR analysis of genomic DNA from cultures obtained. A complete list of strains used is given in Supporting Information, Table S5.

The *his-3* marker was placed in *Δupf1* by crossing RANCR6A *(his-3*, *inl*, *mat a)* (Pratt and Aramayo 2002) with FGSC 11230 (ΔNCU04242, *upf1*, *mat A)* and in *Δupf2* by crossing FGSC6103 *(his-3*, *mat A)* with FGSC15706 (ΔNCU05267, *Δupf2*, *mat a)* with the *his-3* strain serving as the female parent. To rescue the NMD mutations, plasmids designed for *his-3* targeting that contained UPF1, 3XFLAG-tagged UPF1, 3XFLAG-tagged UPF2, or HAT-FLAG-tagged UPF2 were linearized with SpiI and used to transform *Δupf1*, *his-3* or *Δupf2*, *his-3* to histidine prototrophy. Transformation of *N. crassa* by electroporation was accomplished as described previously (Margolin *et al.* 1997; Wei *et al.* 2013).

The rescue of *Δxrn1*, *Δy14*, *Δmago*, *Δcbp20*, and *Δcbp80* mutants was accomplished by ectopic integration with the corresponding functional gene using linearized plasmid DNA that also contained the dominant selectable Bar^r marker. Transformants were selected on the basis of resistance to 250 μg/ml glufosinate (TRC no. G596950) (Pall and Brunelli 1993). Bar^r homokaryotic strains were obtained by microconidiation and the presence of the rescuing transgene confirmed by Southern or PCR analyses of chromosomal DNA.

Luciferase reporters were placed at specific chromosomal sites for analyses of gene expression. Reporters were

integrated at *his-3* by transformation of *his-3* or *his-3 Δupf1* strains. Because *y14* (NCU03226, Supercontig 1: 4971616-4972891 +) was closely linked to *his-3* (NCU03139, Supercontig 1, 4694797-4697762 +), for analyses of reporter activity in *Δy14*, a two-step approach was used for placing the reporter at a different chromosomal position in this strain. First, luciferase constructs were placed at *csr-1* (NCU00726, Supercontig 1, 7404112-7406331 −) by transformation of the wild-type strain (FGSC 2489) with *luc* reporters on linearized plasmids designed for targeting to *csr-1* (Bardiya and Shiu 2007). Disruption of this locus results in resistance to cyclosporin A. The resulting strains containing *luc* at *csr-1* were then crossed with *Δy14* using *Δy14* as the male parent; progeny that contained *luc* and that were either $y14^{+}$ or *Δy14* were used for subsequent analyses. Strains containing *luc* reporters at *csr-1* were also crossed to *Δcbp80* to obtain *luc* reporters in that mutant background; crosses of the resulting strains with *Δcbp20* were used to obtain *Δcbp20 luc* and *Δcbp80Δcbp20 luc* strains. All progeny were purified by microconidiation and genotypes of strains were confirmed by qPCR and PCR. Confirmation of correct polyadenylation and correct splicing of 3′-UTR introns (where relevant) of endogenous *eif4a3*, *erf1*, *y14* transcripts and of *luc-cox5*, *luc-eif4a3+I*, *luc-eif4a3-I* reporters were confirmed by 3′-RACE.

Phenotypic analyses

Phenotypic analyses of *N. crassa* deletion strains and rescued strains were performed as described (Colot *et al.* 2006) with these modifications. Homokaryotic *N. crassa* strains were obtained by isolation of microconidia and grown in either 125-ml flasks with 25 ml Vogel's minimal medium (VM)/1.5% sucrose/2% agar or in 16 × 100-mm glass culture tubes with 3 ml VM/1.5% sucrose/2% agar at 25° with 12:12 hr L:D for 4 days or on 20 ml VM/1.5% sucrose/2% agar or VM/2% yeast extract/1.5% sucrose/2% agar plates at 25° or 37° for 2 days with 12:12 hr L:D. Growth patterns of wt and KO strains were imaged with Canon 50D or 60D digital cameras equipped with Canon EF 50mm f/2.5 macro lenses. Linear growth rates were obtained using race tubes containing 12 ml VM/1.5% sucrose/2% agar at 25° with 12:12 hr L:D for 4 days. Aerial hyphae height was calculated with strains grown with 12:12 hr L:D for 4 days at 25° either with 2 ml VM/1.5% sucrose or VM/2% Yeast Extract/1.5% sucrose. Female sexual development analysis was accomplished by growing strains with 3 ml 1 × SC/1.5% sucrose/2% agar (Westergaard and Mitchell 1947) at 25° with 12:12 hr L:D in 25 ml Falcon tissue culture flasks (Corning Life Sciences DL 353018) with the cap not fully tightened. Scoring for protoperithecia formation and fertilization with FGSC2489 (*74A*) or FGSC4200 (*74a*) were accomplished on day 7, perithecia formation was scored on day 14, and ascus formation was scored on day 21. The time-lapse movies were created by incubating plates at room temperature (a detailed protocol is available upon request).

Plasmid construction

Plasmids designed for rescuing N. crassa deletion mutants: The vectors and oligonucleotides used to create constructs for gene rescue are listed in Table S6. Epitope-tagged genes that could be targeted to the *his-3* locus were made using the vectors pCCG::C-3xFLAG (FJ457001) or pCCG::C-HAT::FLAG (FJ457003) (Honda and Selker 2009). Plasmid pZY05 (*his-3*::$upf1_P$-*upf1*) has the fragment amplified with oYZ165 and oYZ166 containing 750 bp upstream of *upf1* and 3282-bp coding region of *upf1* and 526 bp downstream. The *Not*I/*Eco*RI-digested *upf1* fragment was then inserted to pBM61 (Margolin *et al.* 1997). Plasmid pZY43 (*his-3*::$upf1_P$-*upf1-Gly-3xFLAG*) contains the promoter and coding region of *upf1* amplified by oYZ165 and oYZ194 inserted into pCCGC–Gly3xFLAG (FJ457001) using *Not*I and *Pac*I sites. A shuttle plasmid pZY67 based on a modified pSK− vector (containing an additional *Pac*I site between its *Eco*RI and *Sma*I sites) contains the promoter of *upf2* (970 bp amplified by oZY219 *Not*I/oYZ220 *Spe*I) and coding region of *upf2* (3422 bp amplified by oYZ221 *Spe*I/oYZ222 *Pac*I). This plasmid was used to insert a *Not*I/*Pac*I fragment containing *upf2* into pCCGC–Gly3xFLAG (FJ457001) and pCCGC–GlyHATFLAG (FJ457003) to create plasmids pZY68 (*his3*::$upf2_P$-*upf2-Gly3xFLAG*) and pYZ70 (*his3*::$upf2_P$-*upf2-GlyHATFLAG*), respectively. An *Mlu*I/*Ase*I fragment including 972 bp *xrn1* promoter, 50-bp 5′-UTR, 4565 bp *xrn1* gene, 255-bp 3′-UTR, and 859-bp *xrn1*downstream region (amplified from *N. crassa* genomic DNA with oligo-pair oYZ477/oYZ478) was inserted into pBAR (Pall and Brunelli 1993) to create pZY125 ($xrn1_P$-*xrn1-[Bar^r]*). An *Mlu/Nde*I fragment including 450-bp *y14* promoter, 174-bp 5′-UTR, 628-bp *y14* gene, 474-bp 3′-UTR, and 503 bp *y14* downstream (amplified with oligo-pair oYZ435/oYZ436) was inserted into pBAR to create pZY120 ($y14_P$-*y14-[Bar^r]*). An *Mlu/Nde*I fragment including 1304 bp upstream of *mago*, 59-bp 5′-UTR, 801-bp *mago* gene, 346-bp 3′-UTR, and 1130 bp downstream of *mago* (amplified with oligo-pair oYZ437/438) was inserted into pBAR to create pZY121 ($mago_P$-*mago-[Bar^r]*). An *Mlu/Nde*I fragment including 1045 bp upstream of *cbp80*, 112-bp 5′-UTR, 2766-bp *cbp80* gene, 206-bp 3′-UTR, and 1075 bp downstream of *cbp80* (amplified with oYZ479/oYZ481) was inserted into pBAR to create pZY126 ($cbp80_P$-*cbp80-[Bar^r]*). An *Mlu/Nde*I fragment including 461 bp upstream of *cbp20*, 191-bp 5′-UTR, 771-bp *cbp20* gene, 481-bp 3′-UTR, and 344 bp downstream of *cbp20* (amplified by oYZ501/502) was inserted into pBAR to create pZY128 ($cbp20_P$-*cbp20-[Bar^r]*).

Plasmids designed for placing luc reporters in N. crassa: Vectors and oligonucleotides used to construct luciferase reporters are listed in Table S7. Plasmids pZY78 (*his-3*::*cox-5*$_P$*\cox-5\luc*) and pZY82 (*his-3*::*cox-5*$_P$*\cox-5\luc\cox-5*) containing codon-optimized firefly luciferase was constructed as described (Wei *et al.* 2013). pZY92 (*his-3*::*cox-5*$_P$*\cox-5\luc\eIF4A3+I*) and pZY94 (*his-3*::*cox-5*$_P$*\cox-5\luc\eIF4A3-I*) had the same *cox-5* promoter as pZY82. The 1486-bp 3′ region of *eif4a3* including the intron-containing 3′-UTR was

amplified with oYZ330 and oYZ332 from *N. crassa* genomic DNA template, digested with *Pac*I, and inserted into the pZY78 *Pac*I site. A matched construct containing an intronless 3′-UTR was created by two-step PCR. In the first round, PCR products obtained with (i) oYZ330 and oYZ334 (eIF4A3 intron del Rv), and (ii) oYZ333 (eIF4A3 intron del Fw) and oYZ332 using chromosome DNA as template. In the second-round PCR, the two gel-purified first-round PCR products were used as template and the oYZ330 and oYZ332 primers were used to create the 1264-bp fragment that was digested with *Pac*I to insert into the pZY78 *Pac*I site. pZY84 (*his-3*::*cox-5*$_P$*cox-5**luc**eRF1+I*) was created by inserting the 1703-bp *Pac*I-digested PCR fragment amplified by oYZ181 and oYZ329 to pZY78. pZY86(*his-3*::*cox-5*$_P$*cox-5**luc**eRF1-I*) was generated by inserting a *Pac*I–*Eco*RI fragment of intronless PCR product of oYZ181 and oYZ182 amplified with cDNA as template to pZY84.

For integrating the *luc* reporters at *csr-1*, plasmids pZY122 (*csr-1*::*cox-5*$_P$*cox-5**luc**cox-5*), pZY123 (csr-1::cox-5$_P$\cox-5\luc\eIF4A3+I), and pZY124 (csr-1::cox-5$_P$\cox-5\luc\eIF4A3-I) were created by placing the *Not*I–*Cla*I restriction fragments of pYZ82, pZY92, and pZY94, respectively, that contained the reporter genes into the corresponding sites of plasmid pCSR-1 (Bardiya and Shiu 2007).

Culture conditions for metabolic labeling with 4TU

Conidia for labeling experiments were obtained from cultures in 125-ml flasks containing 25 ml VM/2% sucrose/2% agar (Vogel 1956). Cultures were grown at 30° with 12:12 hr L:D for 7 days. Conidia were harvested by suspension in VM/2% sucrose, filtered through cheesecloth, counted with a hemacytometer, and inoculated into 50 ml VM/2% sucrose in a 125-ml flask at a concentration of 10^7 conidia/ml. Conidia were germinated under constant light at 32° for 6 hr with 150 rpm shaking.

To incorporate 4-thiouracil (4TU), cultures were adjusted to 0.2 mM 4TU (either Sigma 440736-1G or Acros 359930010) from a 1 M stock freshly dissolved in DMSO. After 15 min incubation, uracil (Sigma U0750) was added to a final concentration of 10 mM from a 0.3 M stock prepared in DMSO. Fifteen-milliliter aliquots of each culture were taken at 0, 3, and 10 min and immediately mixed with 7.5 ml VM/2% sucrose/10 mM uracil that had been prefrozen in a 50-ml conical centrifuge tube, and placed on ice. Rapid chilling by mixing with frozen medium stops detectable 4TU incorporation (Figure S3D). Cells were harvested by filtration onto Whatman 541 filter paper, washed with ice-cold sterile water, and cut into ~0.1-g pieces, and each piece was placed into a 2.0-ml conical screwcap tube (Fisher 02-681-344 tube and VWR 89004-362 cap), quick frozen in liquid nitrogen, and stored at –80° prior to RNA isolation.

RNA isolation

Total RNA from frozen cells was isolated as described (Wei *et al.* 2013). RNA concentration was determined using a Nanodrop spectrophotometer and quality assessed by denaturing gel electrophoresis in formaldehyde gels and northern analyses (Wei *et al.* 2013). Poly(A) mRNA was purified using the Poly(A) Purist MAG kit.

3′-RACE

3′-RACE was accomplished as described (Wei *et al.* 2013) using specific Nest oligos and Nested Universal Primer (NUP) oligo oYZ294 (oligos are listed in Table S8). The second-round PCR products were examined by electrophoresis in 2% TAE agarose gels and the fragments were excised from gels and sequenced.

Southerns and Northerns

Genomic DNA was prepared and Southern analyses were performed as described (Wu *et al.* 2009). Northerns were performed as described (Sachs and Yanofsky 1991) except that dextran sulfate was omitted from the hybridization buffer. The oligonucleotide sequences and templates used to produce PCR fragments to generate probes are listed in Table S9. Predicted sizes of PCR fragments were computed using SeqBuilder of DNASTAR (v. 11.2.1). ^{32}P-labeled probes were generated from PCR fragments by random priming (Feinberg and Vogelstein 1983) followed by clean-up with Sephadex G-50 Quick spin columns (Roche 11 273 973 001).

Biotinylation and purification of 4TU RNA

Biotinylation of 4TU-labeled total RNA (150-μg input) was performed by modification of the published method (Cleary *et al.* 2005). RNA (0.2 μg/μl) and biotin–HPDP (Pierce 21314, 0.2 μg/μl) in 10 mM Tris–HCl pH 7.5, 2 mM EDTA were incubated for 1.5 hr at room temperature in foil-wrapped Eppendorf tubes with end-over-end rotation (New Brunswick TC-6 tube rotator, 10 rpm). The reaction mixtures were extracted twice with an equal volume of chloroform at room temperature to remove unreacted biotin–HPDP. The biotinylated RNA was precipitated by adding 1/10 volume 5 M NaCl and an equal volume of isopropanol, followed by freezing at −80° for at least 1 hr and centrifugation at 16100 × *g* at 4° for 20 min in an Eppendorf 5415R centrifuge. The pellet was washed twice with 80% ethanol and the nucleic acid was resuspended in 100 μl autoclaved and filtered DEPC-treated water.

4TU RNA was purified using Neutr Avidin agarose (Thermo Scientific PI29204). For each 150 μg of biotinylated RNA, Neutr Avidin (150 μl 50% slurry) was equilibrated three times with 250 μl binding buffer (25 mM HEPES–NaOH pH 7.2 and 150 mM NaCl) using a Pierce 89879 spin column and repetitive centrifugations at 500 × *g* for 1 min at room temperature (Eppendorf 5415R). Then biotinylated RNA (1 μg/μl in binding buffer) was added to the settled resin in the column. After 15 min, the column was centrifuged at 500 × *g* for 1 min and the eluted material reapplied to the column and incubated another 15 min. The column was centrifuged again, the flow through discarded, and the column containing the biotinylated RNA washed five times with 250 μl Binding Buffer. The 4TU RNA was eluted by two applications of 150 μl 0.1 M DTT in water and centrifugation. All of these steps were at

room temperature. Eluted 4TU RNA (300 μl) was precipitated by adding 1/10 volume of 3M sodium acetate and 2.5 volumes of 100% ethanol, freezing at −80° overnight, and pelleting by centrifugation at 4° 16000 × *g* for 60 min. Pellets were washed twice with 80% ethanol, air dried, and resuspended in 10 μl sterile filtered DEPC treated water. The RNA was quantified using 0.5 μl of material for NanoDrop spectrophotometry. Recovery of 4 TU-RNA was typically 0.5–1% of total RNA input.

ECL detection of biotinylated 4TU-labeled RNA

Biotinylated RNA was either directly dot blotted onto nylon membrane (Bio-Rad Zeta-Probe Blotting membranes no. 162-0159) or was transferred following denaturing agarose-gel electrophoresis. After rinsing the membrane twice for 5 min with PBS, the membrane was incubated with 1000-fold diluted ECL Streptavidin-HRP Conjugate reagent (Amersham RPN 1231V) in PBS buffer for 5 min and washed twice with PBS for 15 min. The excess liquid was removed and the membrane was incubated 2 min with ECL Western blotting detection reagents (Amersham RPN2106) and detected with a UVP Bioimaging system (HAMAMATSU Digital camera C8484-03G).

cDNA synthesis and quantitative PCR from cDNA (RT- qPCR)

For DNase I treatment in a 10-μl reaction volume, 10 μg total RNA or 0.5 μg 4TU RNA in 1× DNase I buffer was incubated at 37° for 30 min with 1 unit DNase I (Ambion AM1907). The reaction was stopped with 1 μl inactivation resin (Ambion) at room temperature for 2 min and the resin-free supernatant obtained by centrifugation according to the manufacturer's directions. Nucleic acid concentrations were determined by NanoDrop spectrophotometry. DNase I treated total RNA (1 μg) or 4TU RNA (0.2 μg) was used as template to synthesize first-strand cDNA with a combination of oligo$(dT)_{18}$ and random hexamer primers in a 10-μl final reaction volume as described (Wei *et al.* 2013). For RT–qPCR, first-strand cDNA (from 8 ng RNA for mRNA measurement and 0.125 ng RNA for *25S* rRNA measurement) was used for qPCR as described (Wei *et al.* 2013). Oligonucleotides used for qPCR are listed in Table S10.

mRNA half-life analysis

Time points were obtained for triplicate cultures. For each individual culture, the 4TU mRNA/*25S* rRNA ratio at time 0 was set at 1, and the mRNA/25S rRNA ratios at subsequent sampling times normalized to time 0. Half-lives and R^2 values were determined by analysis with GraphPad Prism6 software using a nonlinear regression curve-fit for exponential one-phase decay with the plateau value set to 0.

Luciferase assays

Extracts were prepared as described (Luo *et al.* 1995), quick frozen in aliquots, and stored at −80°. Protein concentration was determined by Bradford assay by mixing 10 μl of serially diluted BSA standards or cell extracts with 150 μl Coomassie Plus Protein Assay Reagent (Thermo Scientific 23236) and absorbance measured with a VICTOR3 V Multilabel Counter (PerkinElmer model 1420) using 96-well plates (Nunclon 167008). Luciferase activity was measured using a VICTOR3 V Multilabel Counter (PerkinElmer model 1420) by mixing 10 μl of samples with 5 μl 5× passive lysis buffer (Promega) and 10 μl firefly luciferase assay reagents (25 mM glyclglycine, 15 mM potassium phosphate solution pH 8.0, 15 mM $MgSO_4$, 4 mM EGTA, 2 mM ATP, 1 mM DTT, 0.1 mM CoA, and 0.075 mM luciferin) (Dyer *et al.* 2000). Luciferase activity was normalized to protein amount and relative *luc* mRNA level.

N. crassa cell free translation

N. crassa translation extracts were prepared from wt and used as described (Wu *et al.* 2007) with *N. crassa* RNA or synthetic capped and polyadenylated mRNA encoding firefly luciferase (Wei *et al.* 2012).

Immunopurification of RNA with antibody against human Y14

For each immunopurification, 120 μl (3.6 mg) of a suspended slurry of Dynabeads Protein G (Invitrogen 100.03D) was pre-equilibrated by washing three times with 200 μl buffer B (10 mM Tris-HCl, pH 8.0, 150 mM NaCl, 2.5 mM $MgC1_2$, 1% NP40) and the beads resuspended with 120 μl of buffer B. *N. crassa* cell extracts were prepared by adding 200–300 mg of −80° frozen mycelia to 1 g baked (>2 hr at 180°) 0.5-mm zirconia/silica beads (BioSpec 11079105z) and 300 μl of buffer A [10 mM Tris-Cl, pH 8.0, 150 mM NaCl, 0.1% Triton-X100, 2.5 mM $MgC1_2$, 1 mM phenylmethylsulfonyl fluoride (PMSF), 10 mM vanadyl ribonucleoside complexes (VRC)]; beads and buffer were prechilled on ice in 0.5-ml screwcap tubes (VWR 16466-034). Cells were broken with a Mini-Beadbeater-16 (Biospec) for two cycles of 1 min at full speed with a 1-min rest interval on ice. A hole was poked in the bottom of the tube with a hot needle and the tube placed inside a 2-ml screwcap tube (Fisher 02-681-344) and centrifuged for 1 min at 16,000 × *g* at 4° and the small tube with the retained beads was discarded. The crude cell extract was then clarified by centrifugation at 4° for 10 min at 16,000 × *g*. Protein concentrations were measured by Bradford assay and adjusted to 3 mg/ml using buffer A and samples held on ice. Each extract (250 μl) was preincubated with 20 μl preequilibrated Dynabeads at room temperature for 10 min with gentle rotation and the extract without the beads was transferred to a fresh tube containing 100 μl Dynabeads and 5 μl of 0.66 mg/ml anti-Y14, clone 4C4 monoclonal antibody (Millipore 05-1511, Lot no. 05-1511); the Dynabeads/antibody had also been preincubated at room temperature for 10 min with rotation. Extract, beads, and antibody were then incubated for 0.5 hr at 4° with gentle rotation. Beads were collected and washed three times with 200 μl of buffer B per wash; beads were suspended in 0.5 ml RNA extraction buffer. RNA was prepared as described (Wei *et al.* 2013), dissolved in 10 μl of water, and DNase I treated, and RNA concentrations were determined by NanoDrop spectrophotometry; 150 ng of each

RNA was used for cDNA synthesis and the amounts of mRNA relative to input (total RNA extracted from the same cells) were determined by RT–qPCR.

Data analysis

The FunCat database (Ruepp *et al.* 2004) was used to calculate functional enrichments for the products specified by the 31 identified mRNAs with spliced 3′-UTR introns through queries at http://mips.helmholtz-muenchen.de/funcatDB/ using the *N. crassa* (TaxId:5141) to p3_p13841_Neu_crass_MIPS containing 10067 annotated genes. Of 31 genes, 28 could be identified in the database; NCU03491 (RNA Splicing factor Pad-1, Broad Funcat as 11.02.03 mRNA synthesis and 11.04.03.01 Splicing), NCU10500 (F-box domain-containing protein), NCU11426 (short chain oxidoreductase) were not identified.

Results

N. crassa NMD mutations increase the levels and stability of mRNAs that are NMD targets

The genes specifying *N. crassa* UPF1 and UPF2, as well as other factors selected on the basis of their importance for controlling mRNA stability in NMD-related pathways in other organisms, could be identified on the basis of sequence similarities to homologs in other organisms (Table S1 and Figure S1). *N. crassa Δupf1* (NCU04242) and *Δupf2* (NCU05267) strains had defects in growth and development when cultured in flasks, slants, plates, or race tubes (Figure S2, Table S2, and File S1). The effect of these mutations on mRNA levels for selected genes that had uORFs or spliced 3′-UTR introns (Figure 1A) was examined by Northern analysis (Figure 1B). When compared to the wild-type strain (wt), levels of *arg-2*, *eif5*, *eif4a3*, and *erf1* mRNA, but not *cox-5* mRNA, increased in *Δupf1* and *Δupf2*. *arg-2* contains an evolutionarily conserved uORF specifying the arginine attenuator peptide (AAP) that causes ribosomes to arrest at the uORF stop codon in response to arginine (Wei *et al.* 2012 and references therein). Ribosome arrest at the homologous *S. cerevisiae CPA1* uORF termination codon was demonstrated to trigger NMD (Gaba *et al.* 2005). *N. crassa eif5* contains two uORFs, which by analogy to their functions in the homologous mammalian transcripts are predicted to have roles in eIF5 autoregulation (Loughran *et al.* 2012). The *N. crassa eif4a3*, *erf1*, and *y14* transcripts each contain a 3′-UTR intron that was efficiently spliced in wt and all mutants examined here (Figure 1C). Such introns downstream of termination codons could trigger NMD via the EJC if a similar system to that operating in higher eukaryotes were present in *N. crassa*. The *cox-5* transcript lacks features that would be expected to trigger NMD and was used as a negative control. The effects of *Δupf1* on growth phenotypes and mRNA levels were corrected by expressing UPF1 (either wild-type UPF1 or UPF1 containing a C-terminal 3XFLAG) from a gene placed at the *his-3* locus (Figure 1B, Figure S2, and File S1). Similarly, placing a gene specifying C-terminally tagged UPF2 at *his-3* corrected the observed *Δupf2* defects (Figure 1B, Figure S2, and File S1). *N. crassa Δupf3* (NCU03435) did not show as pronounced effects as *Δupf1* or *Δupf2* on growth (Table S2) or mRNA levels (Figure 1B). The reason for this is unclear, but the effects of loss of UPF3 activity in mammals on mRNA stability can be different than loss of UPF1 activity (Chan *et al.* 2007), and this mutant was not examined further.

To determine whether *Δupf1* and *Δupf2* directly affected mRNA stability, we first established conditions to metabolically label RNA with 4TU and to perform pulse–chase analyses by pulse-labeling RNA with 4TU and chasing with excess uracil (Figure 2A). 4TU pulse–chase avoids complications from shutting down transcription. 4TU is converted to 4-thiouridine monophosphate by uracil phosphoribosyl transferase [encoded by *N. crassa uc-4* (Buxton and Radford 1982)], converted to the triphosphate, and then incorporated into RNA (Cleary *et al.* 2005). 4TU-RNA can be biotinylated, captured by interaction with avidin, and recovered after reversing linkage to the biotinylation reagent. The capacity to incorporate 4TU into RNA was assessed in wt *N. crassa* and *Δuc-4* (NCU01446). Only wt cells labeled with 4TU gave a strong signal over background (Figure S3, A and B). As expected, new transcription was necessary to obtain 4TU-labeled RNA: preincubation with the general transcription inhibitor thiolutin, which has been shown to decrease transcription in *N. crassa* (Hoyt *et al.* 2000; Lee *et al.* 2009), severely reduced 4TU incorporation, as did chilling cells on ice (Figure S3, C and D). Incorporation of 4TU into RNA rapidly diminished when excess uracil was added to cultures (Figure S3E) and 4TU itself had minimal impact on *N. crassa* growth under the experimental conditions used (<30 min incubation) or during growth for extended periods (Figure S3F), similar to its minimal effects on growth in *S. cerevisiae* (Munchel *et al.* 2011) and *S. pombe* (Sun *et al.* 2012). Furthermore, purified 4TU RNA, unlabeled total RNA and unlabeled poly(A) mRNA programmed the synthesis of [^{35}S]Met-labeled polypeptides with similar distributions of masses in *N. crassa* cell-free translation extracts (Figure S3G). We therefore examined *N. crassa* mRNA stability by pulse-labeling cells for 15 min with 0.2 mM 4TU added to the growth medium followed by the addition of a 50-fold molar excess of uracil directly to growth medium. This procedure quickly and effectively reduced 4TU-labeling of new RNA for the time-frame of our analyses, streamlined parallel analyses of multiple cultures, and avoided potential complications arising from switching cells from conditioned to fresh medium.

We examined the effects of *Δupf1* and *Δupf2* on mRNA levels and stability. Figure 2 compares the level and stability of mRNAs in wt and *Δupf1* cells, and wt cells to which cycloheximide (CYH) was added after 4TU labeling but before the uracil chase was started. CYH blocks eukaryotic translation elongation and in previous studies stabilized NMD-targeted mRNAs (Herrick *et al.* 1990; Carter *et al.* 1995; Zhang *et al.* 1997; Saul *et al.* 2009). In Northern analyses of total RNA in CYH-treated wt cells, levels of *arg-2* and *eif4a3* increased substantially, and *cox-5* increased slightly (Figure 2B). Levels of *arg-2* and *eif4a3*, but not *cox-5*, increased in *Δupf1*. Pulse–chase analyses with 4TU showed that *arg-2*, *eif4a3*, and *cox-5* decayed with first-order kinetics in untreated wt cells (Figure 2C).

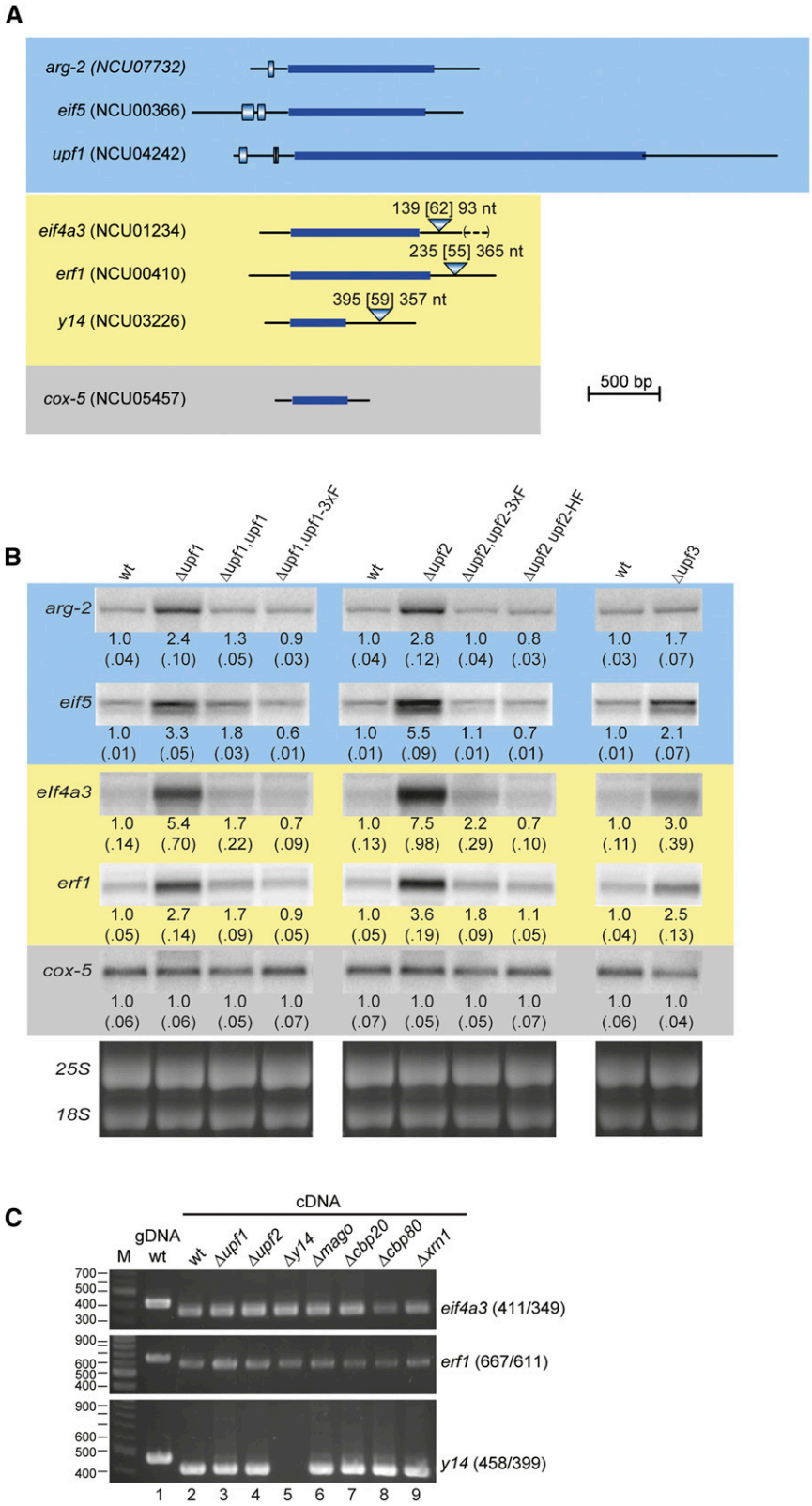

Figure 1 Analyses of uORF-containing and spliced 3′-UTR-containing transcripts. (A) Structures of mRNAs specifying *arg-2*, *eif5*, *upf1*, *eif4a3*, *erf1*, *y14*, and *cox-5*. The solid bars indicate the genic coding regions; the bars with gradients depict uORFs; the triangles indicate the positions and sizes of 3′-UTR introns (no other intron positions are indicated). The distance between the ORF stop codon and the splice site, the size of the spliced intron, and the distance between the splice site and the major poly(A) site are given [*e.g.*, for *eif4a3*, 139, (62), 93 nt]. Here and throughout, shading indicates mRNA features: blue, uORFs that trigger NMD; yellow, spliced 3′-UTRs that trigger NMD; gray, no NMD-triggering features. An extended form of the spliced *eif4a3* mRNA (Figure S4C) contains an additional 87 nt (indicated by dashed lines between parentheses). (B) Northern analyses of wt, *Δupf1*, *Δupf1 his-3*::*upf1*, *Δupf1 his-3*::*upf1-3XFLAG*, *Δupf2*, *Δupf2 his-3*::*upf2-3XFLAG*, *Δupf2*, *his-3*::*upf2-HAT-FLAG*, and *Δupf3*. Total RNA (3 μg/lane) was analyzed with radiolabeled probes for *arg-2*, *eif4a3*, *erf1*, *eif5*, and *cox-5*. Levels of mRNA were quantified and normalized to the level of *cox-5* mRNA. The quantification shown below the bands represents the average and standard deviation from three independent growth experiments. *25S* and *18S* rRNA bands stained with ethidium bromide from representative gels are shown below the Northerns. The doublet for the intronless *eif5* transcript likely represents mRNA isoforms. (C) *eif4a3*, *erf1*, and *y14* 3′-UTR introns are efficiently spliced in all strains examined. M, markers; gDNA, PCR products of genomic DNA template; cDNA, PCR products from cDNA templates. The predicted sizes of PCR products from different templates are indicated. The *Δy14* strain lacks *y14* mRNA. See also Figure S1 and Figure S2.

The stability of *arg-2*, *eif4a3*, *erf1*, *eif5*, and *cox-5* in wt cells increased when cells were treated with CYH (Figure 2C). This indicates that CYH was not affecting NMD substrates specifically, but was acting generally on all mRNAs examined; a mechanism by which it can do so is to inhibit decapping and thus inhibit mRNA degradation (Beelman and Parker 1994). In *Δupf1*, the stability of *arg-2*, *eif4a3*, *erf1*, and *eif5*, but not *cox-5*, increased compared to wt cells as determined

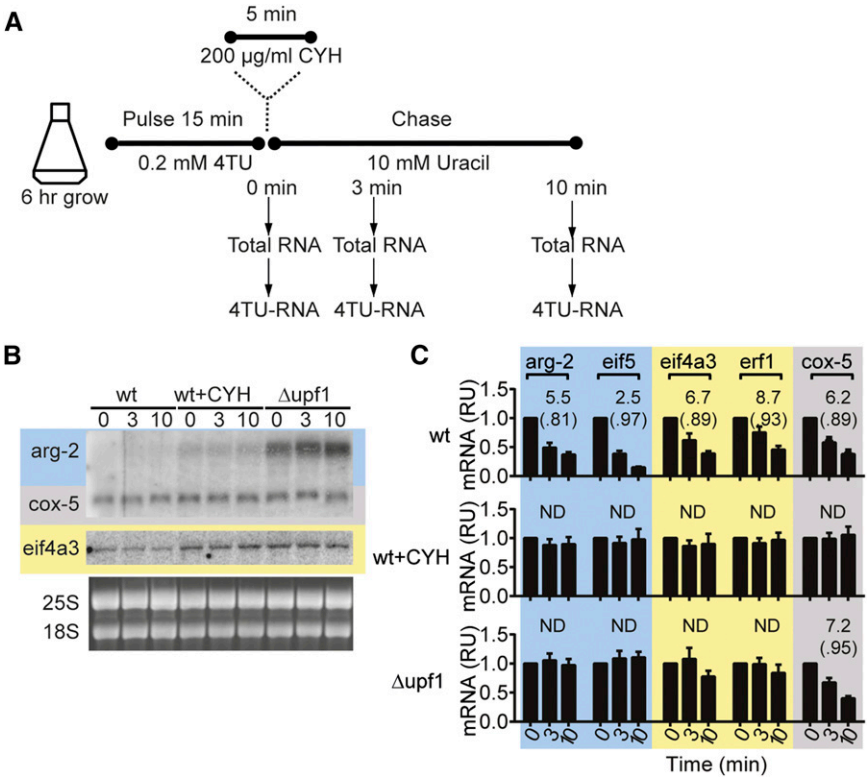

Figure 2 mRNA levels and mRNA stability are affected by growth in cycloheximide and by *Δupf1*. (A) Strategy for pulse–chase analyses of mRNA stability. *N. crassa* conidia were germinated and grown for 6 hr; 0.2 mM 4TU was then added. After 15 min incubation with 4TU, 10 mM uracil was added to the culture, and total RNA and 4TU–RNA was purified from samples taken at 0, 3, and 10 min. In one experiment, cycloheximide (CYH) was added after the 15-min 4TU-pulse; following 5 min of incubation with CYH, the uracil-chase was then performed. (B) Total RNA from wt, *Δupf1*, and wt cells treated with 200 μg/ml CYH and subjected to 4TU pulse–chase were analyzed by Northern blotting as in Figure 1B; the *arg-2* and *cox-5* probes were added together. (C) Pulse–chase analyses of 4TU RNA from wt, *Δupf1*, and CYH-treated wt. 4TU RNA was purified and quantified by RT–qPCR and levels of 4TU mRNAs for *arg-2*, *eif5*, *eif4a3*, *erf1*, and *cox-5* were normalized to levels of 4TU-labeled *25S* rRNA in each sample (4TU-labeled *25S* rRNA is stable during a 10-min chase) and then normalized to the level at time 0. Differences in expression are shown in relative units (RUs). The results are the average of three independent experiments. The mRNA half-lives (in minutes), calculated by fitting data to first order-decay parameters, are shown, as are R^2 values for each calculation (in parentheses). ND, not determined. See also Figure S3.

by pulse–chase analysis (Figure 2C and Figure 3A). Thus, consistent with studies in other organisms, adding CYH to cultures stabilized mRNA, and the *Δupf1* mutation stabilized mRNAs that contained features predicted to make them direct targets of NMD. The effects of *Δupf2* on the stability of *arg-2*, *eif4a3*, *erf1*, and *eif5* (Figure 3B) were similar to those of *Δupf1*, indicating that these transcripts are direct targets of NMD. Introduction of functional copies of *upf1* and *upf2* into the corresponding *Δupf1* and *Δupf2* strains reduced the stability of *arg-2*, *eif4a3*, *erf1*, and *eif5* transcripts to near wild-type levels and largely restored the mutant growth phenotypes, as expected if these phenotypes were direct consequences of the deletion mutations (Figure 3 and Figure S2).

We next examined the consequences of disrupting the predicted *N. crassa* homolog of XRN1 (NCU06678; see Table S1). XRN1 specifies an evolutionarily conserved 5′–>3′ exonuclease important in general mRNA degradation (Hsu and Stevens 1993; Nagarajan *et al.* 2013). We examined the *Δxrn1* strain to establish whether loss of this 5′–>3′ exonuclease had generalized stabilizing effects on mRNA to provide a necessary context for interpreting subsequent analyses of the functions of NMD, EJC, and CBC components on specific mRNAs. The *N. crassa Δxrn1* strain had growth and developmental defects (Figure S2 and Table S2) and stabilized the mRNAs we examined by metabolic labeling with 4TU (Figure 4A). Relative to the wild-type strain, levels of each mRNA were also increased in the mutant (Figure 4B). The growth and mRNA phenotypes were rescued by transforming the *Δxrn1* mutant with the wild-type *xrn1* gene (Figure S2 and Figure 4). These data indicate that XRN1-dependent mRNA degradation is also important in *N. crassa* for determining mRNA stability.

The arg-2 uORF and 3′-UTR introns of eif4a3 and erf1 confer NMD-control to a reporter transcript

We hypothesized that the *arg-2* uORF and the loading of an EJC at the *eif4a3* and *erf1* 3′-UTR introns were responsible for triggering NMD of each respective mRNA. To test this, we introduced these elements into firefly luciferase *(luc)* reporter constructs. We created wild-type *upf1* and *Δupf1* strains harboring *luc* reporters integrated at the *his-3* locus (Figure S4A). One matched set of reporters contained either the *arg-2* uORF specifying the wild-type AAP (AAP_{wt}–luc) or the mutated D12N AAP (AAP_{D12N}–luc), which eliminates the AAP's capacity to cause ribosome arrest at the uORF stop codon (Wei *et al.* 2012 and references therein). Another matched set of reporters produced *luc* mRNAs with the 3′-UTRs of *cox-5*, *eif4a3*, or *erf1*. Reporters whose 3′-UTRs either contained or lacked the *eif4a3* and *erf1* 3′-UTR introns were constructed (Figure S4A). Analyses of total RNA and 4TU pulse–chase data showed the importance of the *arg-2* uORF and the 3′-UTR introns of *eif4a3* and *erf1* in controlling mRNA stability (Figure 5, A–C). Only the reporter transcripts containing the wt AAP or the spliced *eif4a3* or *erf1* 3′-UTR introns were stabilized in *Δupf1* mutant. The 3′-UTRs of reporter mRNAs were mapped by 3′-RACE and showed (i) intron-containing and intron-less reporters were polyadenylated at the sites predicted from the endogenous genes and (ii) the introns were correctly spliced (Figure S4C). The efficiency of translation of each of the mRNAs was compared by measuring LUC enzyme activity in cell extracts and normalizing activities to

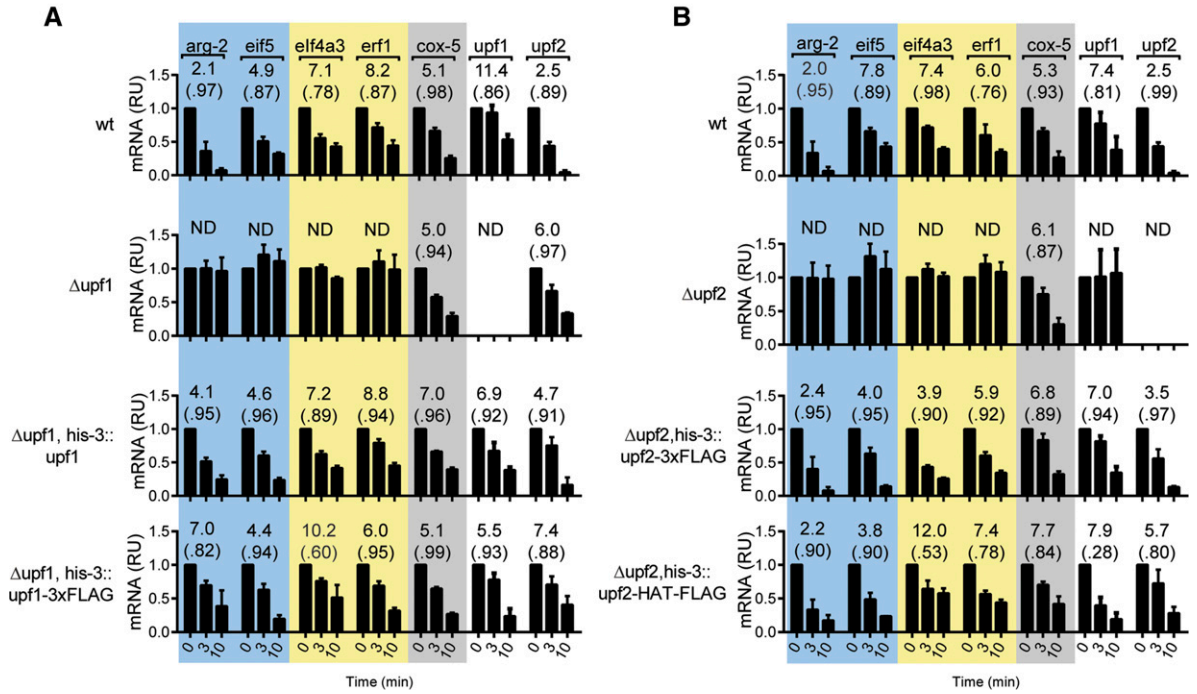

Figure 3 Effects of *Δupf1*, *Δupf2* mutations and correction of these mutants on the stability of selected mRNAs. 4TU RNA from wt, *Δupf1*, *Δupf1 his-3*::*upf1*, *Δupf1 his-3*::*upf1-3XFLAG* strains (A) or *Δupf2*, *Δupf2 his-3*::*upf2-3XFLAG* and *Δupf2*, *his-3*::*upf2-HAT-FLAG* strains (B) were analyzed by pulse–chase for *arg-2*, *cox-5*, *upf1*, *upf2*, *eif4a3*, *erf1*, and *eif5* mRNAs using the procedures described in Figure 2. See also Figure S6.

luc mRNA levels. Neither the 3′-UTR intron of *eif4a3* or *erf1* substantially affected translation efficiency (Figure 5, B and C).

Deletions of EJC components increase the levels and stability of mRNAs that contain 3′-UTR introns

Three of the major components of the EJC are eIF4A3, Y14, and Mago (Table S1). The *N. crassa Δeif4a3* mutant was not viable: *Δy14* grew slowly and had developmental abnormalities; *Δmago* also displayed growth and development defects but these were not as severe as those of *Δy14* (Figure S2, Table S2, and File S1). Overall, mRNA transcript levels in total RNA preparations appeared higher in *Δy14* and *Δmago* than in wt when examined by Northern analysis (Figure 6A) and by RT–qPCR (see Figure 7A). In *Δy14* and *Δmago*, the stability of *eif4a3* and *erf1* transcripts, which contain 3′-UTR introns, increased, but the stability of *arg-2*, *eif5*, and *cox-5* transcripts did not (Figure 6B). Thus while increased levels of transcripts in *Δy14* and *Δmago* might reflect altered transcription levels in addition to increased transcript stability, increased RNA stability was observed only for transcripts containing spliced 3′-UTR introns. Reintroduction of functional *y14* and *mago* genes into the respective strains largely restored the observed defects of the mutants (Figure 6, A and B, Figure S2, and File S1).

The eIF4A3 3′-UTR intron confers mRNA-stability control through the EJC component Y14

If *N. crassa y14* is involved in NMD-mediated control of mRNA stability mediated by an EJC deposited downstream of a termination codon, then the stability of a reporter containing the *eif4a3* 3′-UTR intron but not a reporter lacking the 3′-UTR intron should be increased in the *Δy14* strain. While *his-3* is routinely used for site-specific integration of reporters in *N. crassa*, including the reporters used to study the effects of NMD mutations described above, *his-3* and *y14* are tightly linked chromosomal loci. We therefore integrated *luc* reporter constructs at the *csr-1* locus, which is not closely linked to *y14* (Figure S4B) and crossed these reporter strains to *Δy14* to obtain sibling strains containing each reporter and either wild-type *y14* or *Δy14* alleles to test the impact of *Δy14* on the matched reporter constructs.

Δy14 affected the stability of the *luc* reporter with the intron-containing *eif4a3* 3′-UTR, but not reporters with the intronless *eif4a3* 3′-UTR or *cox-5* 3′-UTR (Figure 7A). In the wild-type strain, the stabilities of all of the reporter mRNAs were similar. Analyses by 3′-RACE showed the reporter transcripts containing the intron were correctly spliced and polyadenylated (Figure S4C). As expected, the stability of the endogenous *eif4a3* transcript also was increased in *Δy14* but not wt (Figure 7A). Measurements of translational efficiency indicated that the presence of the *eif4a3* 3′-UTR intron decreased translation efficiency in both the wild-type and *Δy14* strains (Figure 7A), arguing against the possibility that increased translation of the spliced mRNA accounts for its instability. These data (Figure 6B and Figure 7A) indicate that *Δy14* is specifically affecting the stability of transcripts that contain 3′-UTR introns.

Mutations eliminating nuclear cap-binding complex components CBP20 and CBP80 increase the levels and stability of mRNAs that contain 3′ UTR introns

In higher eukaryotes, CBP20 and CBP80, which form the nuclear CBC, affect the stability of transcripts that contain an

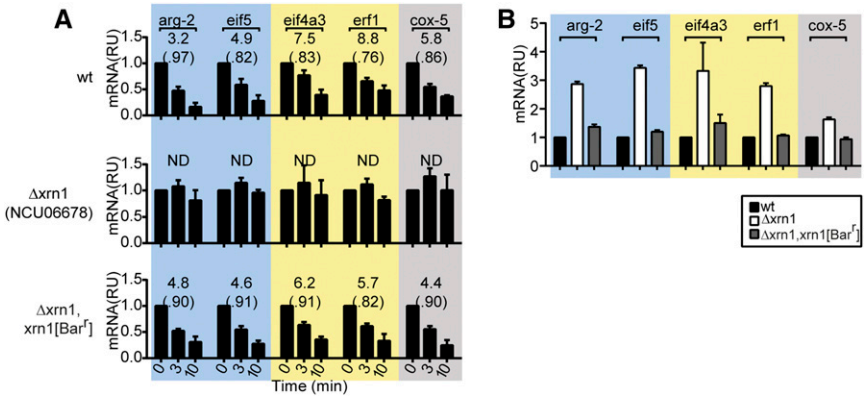

Figure 4 Effects of *Δxrn1* and correction of the mutant on the stability of selected mRNAs. (A) 4TU RNA from wt, *Δxrn1*, and *Δxrn1 xrn1*[*Bar*^{r}] strains were analyzed by pulse–chase for *arg-2*, *eif5*, *eif4a3*, *erf1*, and *cox-5* mRNAs using the procedures described in Figure 2. (B) Levels of mRNA in total RNA from wt, *Δxrn1*, and *Δxrn1 xrn1*[*Bar*^{r}] strains was quantified by RT–qPCR and mRNA levels were normalized to the level of *25S* rRNA.

intron downstream of the native termination codon (Hwang *et al.* 2010; Popp and Maquat 2013). Therefore we examined the effects of deleting these factors on the stability of 3′-UTR-intron containing *N. crassa* transcripts. The *Δcbp20* and *Δcbp80* strains had mild growth phenotypes (Figure S2, Table S2, and File S1). Analyses of mRNA stability (Figure 6C) showed that deletion of either *Δcbp20* or *Δcbp80* increased the stability of the 3′-UTR–intron transcripts *eif4a3* and *erf1* but not *arg-2*, *eifi5*, or *cox-5*. The growth defects and the altered stability of *eif4a3* and *erf1* transcripts in the mutant strains were corrected when the strains were rescued with wild-type copies of the genes (Figure 6C, Figure S2, and File S1).

We tested whether the effects of these deletions on mRNA stability was due to the presence of a 3′-UTR intron in the affected genes by examining *luc* reporters with and without the *eif4a3* intron (Figure 7B and Figure S5). Only reporters containing the 3′-UTR intron showed increased stability in the *Δcbp20*, *Δcbp80*, and the *Δcbp20 Δcbp80* double-mutant strains. Measurements of translational efficiency in the *Δcbp80* strain (Figure 7B) indicated that the spliced reporter mRNA was translated with less, not more, efficiency than the intronless reporter, arguing against increased translation of the spliced mRNA accounting for its instability.

The *y14* mRNA also contains a 3′-UTR intron (Figure 1A). Therefore we examined the half-life of this transcript in *Δupf1*, *Δupf2*, *Δmago*, *Δcbp20*, and *Δcbp80* strains and the corresponding rescued strains (Figure S6, A–C). The effects of these mutations and their corrections on *y14* mRNA half-life were similar to the effects observed on *eif4a3* and *erf1* mRNA half-lives, indicating that the *y14* mRNA's spliced 3′-UTR intron also controls this mRNA's stability. The levels of *y14* mRNA in total RNA in the different strains showed a profile similar to the *eif4a3* and *erf1*mRNAs (Figure S6D). Thus, the *y14* mRNA's spliced 3′-UTR intron appears important for NMD; however, it is also possible that the 752-nt 3′-UTR of the major form of the spliced transcript could itself trigger NMD by virtue of its being a long 3′-UTR.

Immunopurification with anti-Y14 antibody enriches for mRNA containing 3′-UTR introns

The stabilities of *N. crassa* mRNAs containing spliced 3′-UTR introns appear controlled through the EJC. Thus it is important to obtain direct evidence whether there is binding of the EJC to mRNAs containing spliced 3′-UTR introns. RT–qPCR was used to examine RNAs that were immunopurified from *N. crassa* extracts using monoclonal antibody directed against human Y14. Enrichment for *erf1*, *eif4a3*, and *y14* mRNA, relative to *arg-2*, *cox-5*, and *eif5* mRNA, was seen when wild-type cells were examined (Figure 7C). Such enrichment was not observed in immunopurifications from the *Δy14* or *Δmago* mutants or from mock immunopurifications from the wild-type strain (Figure 7C). Importantly, in wild-type strains containing *luc* reporters, enrichment was observed for reporters with either *eif4a3* or *erf1* 3′-UTR introns but not from matching reporters lacking 3′-UTR introns (Figure 7D), and enrichment of the endogenous *eif4a3* mRNA relative to the *arg-2* mRNA is observed in all cases. These data indicate that Y14, which is part of the EJC, is associated with mRNAs containing spliced 3′-UTR introns. Taken together with the RNA stability data, this indicates a direct role for the EJC in governing the stability of mRNAs containing spliced 3′-UTR introns.

Discussion

Here we show that the degradation of mRNA through the NMD pathway in the model filamentous fungus *N. crassa* has at least two branches, one requiring the NMD factors and the other requiring EJC and CBC factors in addition to NMD factors. We show that this latter pathway controls the stability of spliced 3′-UTR intron containing mRNAs for the EJC components eIF4A3 and Y14, and the nonsense-codon-sensing termination factor eRF1. The absence of evidence for EJC-mediated NMD in fungi has been discussed (Rebbapragada and Lykke-Andersen 2009; Wen and Brogna 2010; Kervestin and Jacobson 2012); this is the first demonstration of EJC-mediated NMD in fungi. Our results thus establish that this quality-control process controlling mRNA stability has evolutionary and functional conservation. While the importance and necessity for CBC factors in EJC-dependent NMD have been debated (Hosoda *et al.* 2005; Dzikiewicz-Krawczyk *et al.* 2008; Maquat *et al.* 2010; Durand and Lykke-Andersen 2013; Rufener and Muhlemann 2013), our data provide the first demonstration in any system that CBC factors are not only important for, but are essential for, the EJC-dependent branch of NMD.

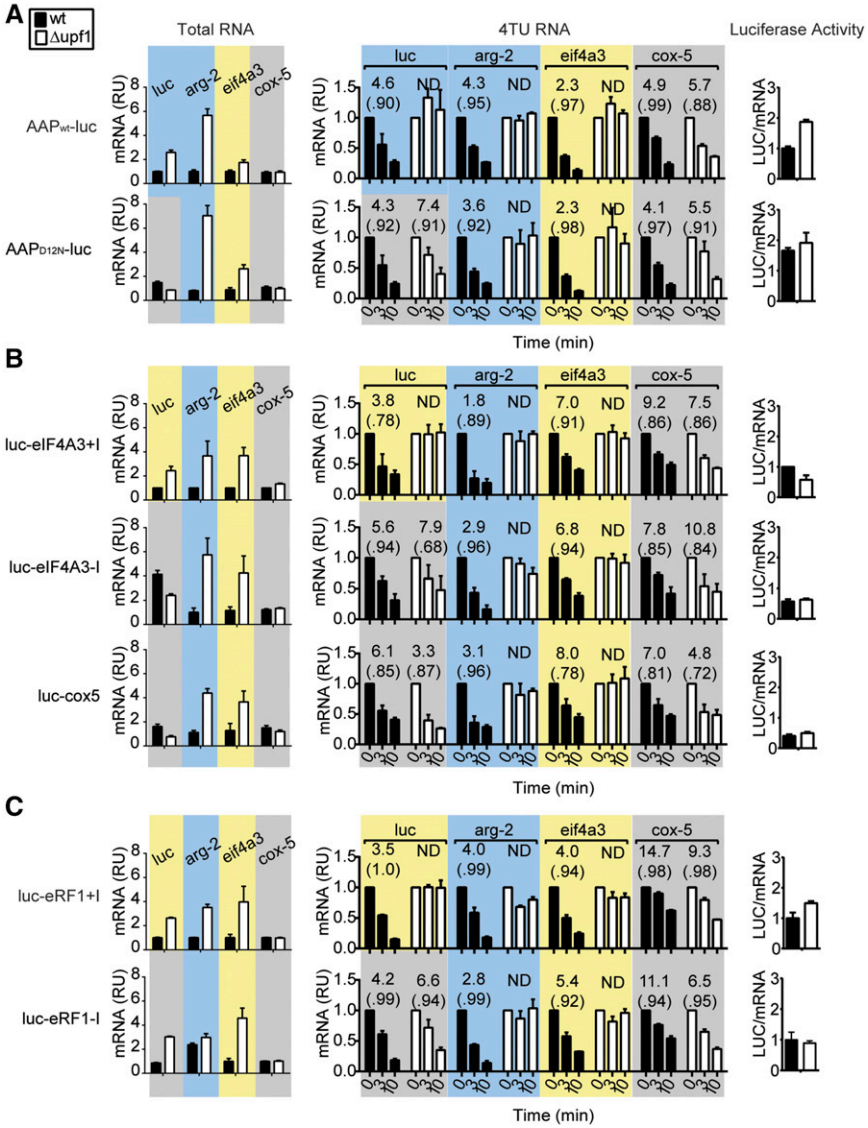

Figure 5 Effects of the *arg-2* uORF-encoded AAP and the *eif4a3* and *erf1* 3′-UTR introns on the level and stability of *luciferase* (*luc*) reporter mRNA in wt and Δupf1 strains. Measurements to analyze the effects on reporter genes containing the *arg-2* uORF (A), the *eif4a3* 3′-UTR intron (B), and the *erf1* 3′-UTR intron (C) and controls are shown as follows for each: levels of mRNA in total RNA (left), half-lives of mRNA measured by 4TU RNA pulse–chase (middle), and levels of luciferase enzyme activity/mRNA (right). wt (solid bars) or *Δupf1* (open bars) strains contained the *luc* reporters shown in Figure S4A. Measurements of RNA were accomplished as in Figure 4. Luciferase enzyme activity was measured and normalized to *luc* mRNA levels. See also Figure S4.

Our results show that *N. crassa* eIF4A3, eRF1, Y14, and UPF1 are subject to autoregulatory control at the level of mRNA stability through pathways involving NMD, EJC, and CBC factors because mutations that eliminate these factors increase the stability of these transcripts. Specifically, *eif4a3* and *erf1* mRNA stability increased in *Δupf1*, *Δupf2*, *Δy14*, *Δmago*, *Δcbp20*, and *Δcbp80* mutants; *y14* mRNA stability increased in *Δupf1*, *Δupf2*, *Δmago*, *Δcbp20*, and *Δcbp80* mutants; and *upf1* mRNA stability increased in the *Δupf2* mutant. The transcripts for two EJC factors (eIF4A3 and Y14) and for termination factor eRF1 each contain a spliced 3′-UTR intron and reporter analyses demonstrated that the spliced *eif4a3* and *erf1* 3′-UTR introns were sufficient to confer control of mRNA stability through NMD-related pathways. Therefore the situation appears analogous to what occurs in higher eukaryotes in which such introns can trigger EJC-mediated NMD. NMD control of *N. crassa upf1* mRNA stability might be exerted through recognition of its uORF stop codons as PTCs, as is the case for *N. crassa arg-2* (Figure 5A) and *S. cerevisiae CPA1* (Gaba *et al.* 2005), or through its relatively long 3′-UTR (Figure 1A) as is reported for metazoan *UPF1* (Huang *et al.* 2011; Longman *et al.* 2013), but this remains to be determined.

To our knowledge, this work represents the first demonstration of circuits that enables regulation at the level of mRNA stability for eRF1, eIF4a3, and Y14. Autoregulation of mRNA levels for NMD factors has been reported for metazoans (Huang *et al.* 2011; Yepiskoposyan *et al.* 2011; reviewed in Karam *et al.* 2013; Longman *et al.* 2013) and autoregulation of NMD and EJC factors has been reported for plants (Nyiko *et al.* 2013). Measurements of mRNA stability in mammalian cells established that UPF2 and SMG1 (a kinase that phosphorylates UPF1) are stabilized in UPF1-depleted cells and that UPF1 is stabilized in SMG1 depleted cells; furthermore the UPF1 3′-UTR conferred UPF1-dependent mRNA stability to a reporter (Huang *et al.* 2011). The long 3′-UTRs of mRNAs specifying UPF1, SMG5, and SMG7 (the latter two proteins affect the dephosphorylation of UPF1)

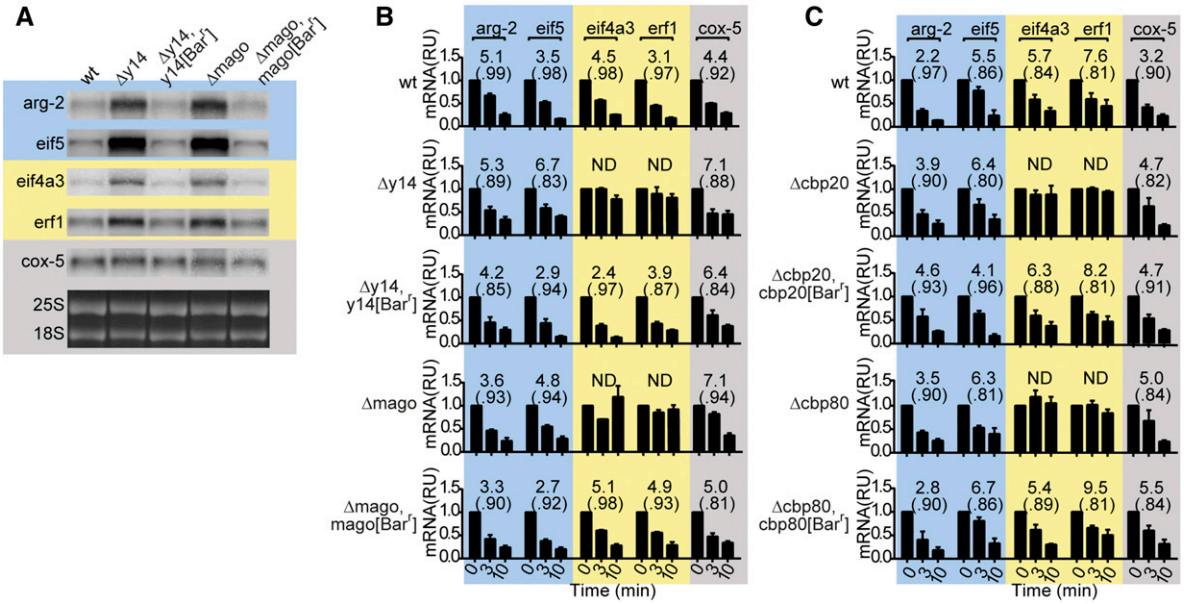

Figure 6 Effects of *Δy14*, *Δmago*, *Δcbp20*, and *Δcbp80*, and correction of these mutants, on the stability of selected mRNAs. (A) Aliquots (3 μg) of total RNA extracted from wt, *Δy14*, *Δy14 y14-Bar*^{r}, *Δmago*, and *Δmago mago[Bar*^{r}*]* were separated on formaldehyde denaturing gels and analyzed as described in Figure 1B with the indicated probes. 4TU RNA from wt, *Δy14*, *Δy14 y14[Bar*^{r}*]*, *Δmago*, *Δmago mago[Bar*^{r}*]* (B) or wt, *Δcbp20*, *Δcbp20 cbp20[Bar*^{r}*]*, *Δcbp80*, *Δcbp80 cbp80[Bar*^{r}*]* (C) was analyzed by pulse–chase for *arg-2*, *eif5*, *eif4a3*, *erf1*, and *cox-5* mRNAs using the procedures described in Figure 2. See also Figure S6.

reduced the relative stability of an mRNA reporter in mammalian cells (Yepiskoposyan *et al.* 2011). The transcript levels for *Arabidopsis* SMG7 and Barentsz/MLN51 (which in higher eukaryotes is another component of the EJC), each contain a spliced 3′-UTR intron (Nyiko *et al.* 2013). Analyses of reporters containing these spliced 3′-UTR introns showed that their mRNA levels were upregulated in *upf1* and *upf3* mutants and that the 3′-UTR introns were at least partially responsible for this alteration in transcript levels; in these studies, mRNA stability was not directly assessed (Nyiko *et al.* 2013).

We confirmed that other filamentous fungi also contained spliced 3′-UTR introns in their *eif4a3*, *y14*, and *erf1* transcripts, indicating evolutionary conservation of these elements. Specifically, analyses using FungiDB (Stajich *et al.* 2012) show 3′-UTR introns in *erf1* in *Fusarium verticillioides* (FVEG_08271), *A. nidulans* (AN8853), and *Magnaporthe oryzae* (MGG_06266); in *eif4a3* in *F. oxysporum* (FOXG_07544), *F. verticillioides* (FVEG_04473), *M. oryzae* (MGG_04885), and *y14* in *N. discreta* (NEUDI_81291), *N. tetrasperma* (NEUTE1DRAFT_149143), and *F. verticillioides* (FVEG_03573). The *erf1* mRNA of the basidiomycete pathogen *Cryptococcus neoformans* (CNAG_02948) also has a 3′-UTR intron (http://www.broadinstitute.org/annotation/genome/cryptococcus_neoformans/MultiHome.html).

The appearance of spliced 3′-UTR introns in *eif4a3*, *y14*, and *erf1* transcripts raises the question of their appearance in other transcripts. Gene models from Release 7 of the *N. crassa* genome indicate that 321 of the 9728 predicted protein coding genes in *N. crassa* potentially have 3′-UTR introns. For 237, the 3′-UTR-intron was present in all predicted transcript models. We examined these 237 transcripts using our recently published RNA-seq data (Wu *et al.* 2014). We obtained clear evidence for a spliced 3′-UTR intron in 31 cases (Table S3). FunCat analyses of these 31 genes indicated enrichment in categories related to DNA, RNA, and protein synthesis as well as other several categories (Table S4). Thus the fraction of genes that produce normal transcripts with spliced 3′-UTR introns appears to be quite low in *N. crassa*, at least in vegetatively growing cultures. In contrast, many *N. crassa* transcripts contain uORFs; based on EST analyses, 22% of *N. crassa* mRNAs are estimated to contain uORFs (Galagan *et al.* 2005).

The *N. crassa* CBC components CBP20 and CBP80 are crucial for the EJC-mediated NMD processes we observed (Figure 6, Figure 7, and Figure S5). The question of whether mRNA must be associated with the CBC for decay to occur has been debated with respect to mammals (Maquat *et al.* 2010; Durand and Lykke-Andersen 2013; Rufener and Muhlemann 2013) and while CBC has been considered important for the process, whether it is essential is also unclear. Examination of *N. crassa* mutants lacking CBP20 and/or CBP80 clearly indicate that the capacity of cells to produce CBC controls the stability of endogenous and reporter transcripts containing a spliced 3′-UTR intron. This directly answers affirmatively the mechanistic question of whether CBC has an essential role for this process. The question of whether in *N. crassa* the CBC must be associated with the mRNA or can be been exchanged for eIF4E prior to the onset of decay is not yet resolved. Importantly in this regard, *N. crassa* CBC is not required for controlling the stability of uORF-containing mRNAs such as *arg-2* and *eif5* whose

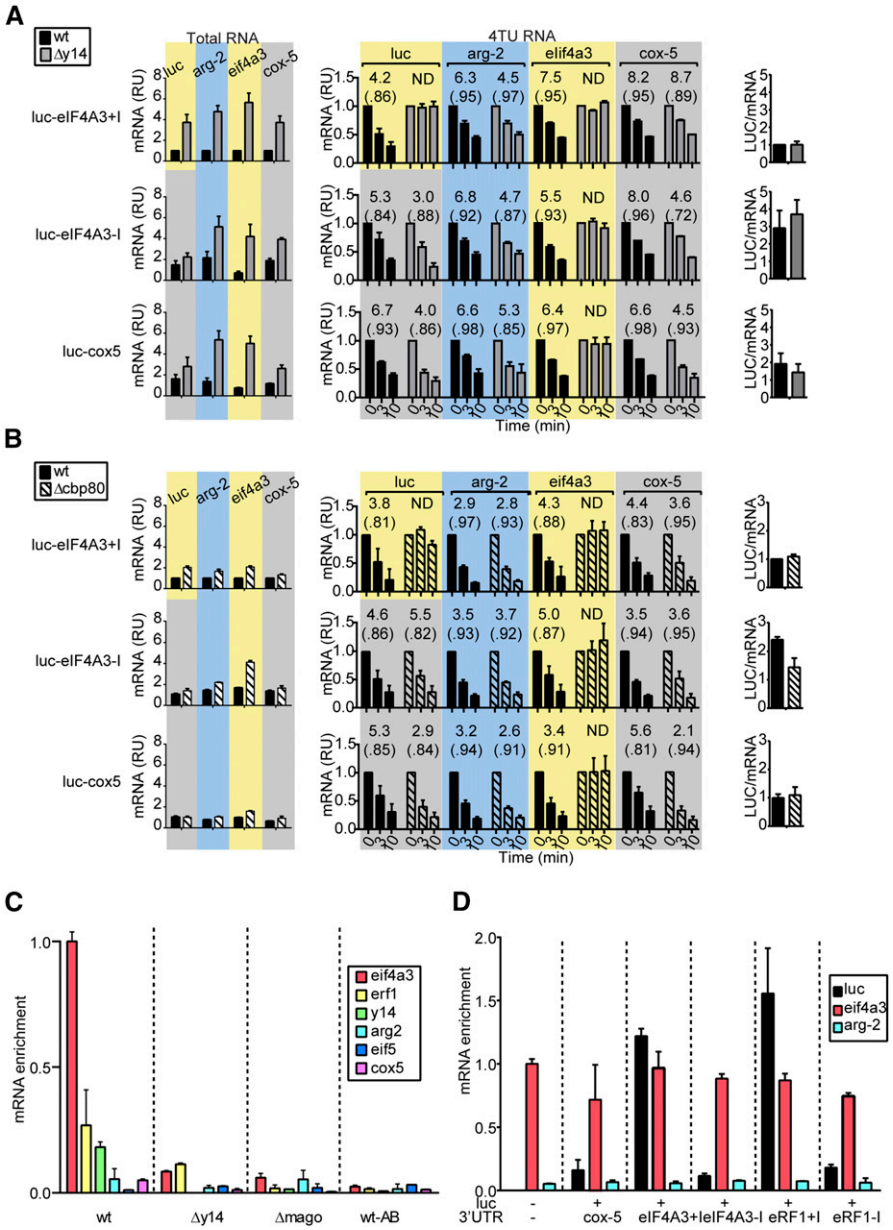

Figure 7 Effects of the *eif4a3* 3′-UTR intron on the level and stability of *luc* reporter mRNA in wt, *Δy14* and *Δcpb80* strains. Measurements to analyze the effects on reporter genes containing the *eif4a3* 3′-UTR intron and controls are shown as follows for each: levels of mRNA in total RNA (left), half-lives of mRNA measured by 4TU RNA pulse–chase (middle), and levels of luciferase enzyme activity/mRNA (right). (A) wt (solid bars) and *Δy14* (shaded bars) strains contained the *luc* reporters shown in Figure S4B. (B) wt (solid bars) and *Δcbp80* (hatched bars) strains contained the *luc* reporters shown in Figure S4B. Measurements were obtained as described in Figure 5. (C) RT–qPCR analysis of *eif4a3*, *erf1*, *y14*, *arg-2*, *eif5*, and *cox-5* mRNAs purified from wt, *Δy14*, and *Δmago* strains by immunopurification of mRNPs with anti-Y14 antibody as described in *Materials and Methods*. The level of each transcript was normalized to the total amount of purified RNA and then normalized to the level of input transcript. Mock immunopurification from wt without antibody (wt-AB) served as the control. (D) RT–qPCR analyses of *luc*, *eif4a3*, and *arg-2* mRNAs purified from wt and *luc* reporter strains by immunopurification of mRNPs with anti-Y14 antibody. mRNA enrichment is shown normalized to the enrichment of *eif4a3* in immunopurification from wt cells. See also Figure S5 and Figure S6.

stability is controlled by NMD factors but not EJC factors. Taken together, these data show that CBC factors are important for producing mRNP that is permissive for EJC-mediated, but not uORF-mediated, NMD. It is increasingly apparent that the nuclear history of a transcript can define its fate in the cytoplasm (Trcek *et al.* 2011; Haimovich *et al.* 2013; Zid and O'Shea 2014), and regardless of whether the CBC or eIF4E is associated with the mRNA at the onset of decay, CBC appears essential for EJC-mediated NMD. Thus, the CBC is critical for licensing EJC-mediated NMD.

The levels of RNAs *(eif4a3*, *erf1*, and *y14)* that are stabilized in CBC mutants do not increase as dramatically in the total RNA pools of these mutants as they do in the EJC mutants (Figure 6A, Figure 7, A and B, and Figure S6D). A possible explanation for this is that the CBC mutants leave autoregulatory circuits intact that enable feedback between transcript levels and transcription for *eif4a3*, *erf1*, and *y14*, so that increased stability decreases transcription. With respect to the EJC and NMD mutants, this circuit might be disrupted or there might be additional transcriptional induction independent of an intact feedback circuit. The existence of such feedback circuits that connect RNA stability and transcription has been demonstrated in *S. cerevisiae* through the functions of XRN1 (Haimovich *et al.* 2013).

All of the viable deletion mutations affecting NMD, EJC, and CBC components displayed asexual growth phenotypes. Some of these mutants also had defects in their sexual development: the *Δy14*, *Δmago*, and *Δupf2* strains are female sterile. The formation of protoperithecia, the earliest female-specific developmental structures in *N. crassa*, is eliminated in *Δy14* and *Δmago* mutants under standard inducing conditions, and *Δupf2* reduces protoperithecium formation. These

data suggest that Y14, MAGO, and UPF2 have additional roles in the sexual cycle genetically distinguishable from their roles in triggering NMD in asexually growing cells. While the bases for these female-specific phenotypes for this subset of factors involved in NMD remain to be determined, it is interesting in this regard that *mago* was originally identified in *Drosophila melanogaster* as a maternal-effect gene affecting oocyte development and subsequent work has established roles for fly Y14 and Mago to correctly position *oskar* mRNA to enable oocyte development (Boswell *et al.* 1991; Hachet and Ephrussi 2001, 2004; Mohr *et al.* 2001; Ghosh *et al.* 2014). We note here that BLAST comparisons that find close homologs in *N. crassa* for Y14, Mago, and eIF4A3 do not detect the EJC component Barentsz/MLN51 (Table S1); whether *N. crassa* contains a functional homolog of Barentsz/MLN51, which has roles in NMD and mRNA positioning (Palacios *et al.* 2004) remains to be determined.

The *N. crassa period-6 (prd-6)* gene was identified to harbor a spontaneous mutation that shortens the period of the fungus's circadian cycle at temperatures above, but not below, 21° (Morgan and Feldman 1997). Unpublished work identified the product of this gene as UPF1 (Compton 2003) and the original *prd-6* allele as a frameshift mutation resulting in a premature termination codon in the UPF1 coding region. The basis for the circadian phenotype of this *upf1* allele, and whether mutations affecting other components of the NMD pathway similarly affect circadian rhythms in *N. crassa*, remain to be determined. More generally, the role of NMD in controlling circadian rhythms has not been documented in other organisms, although there is evidence that alternatively spliced transcripts for some *Arabidopsis* clock genes are degraded by NMD (Kwon *et al.* 2014) and NMD mutants in this organism show alterations in the way photoperiod-dependent genes are expressed (Shi *et al.* 2012).

The use of 4TU in *N. crassa* enabled unprecedented measurements of RNA stability by metabolic labeling. In *N. crassa*, a good fit to first-order decay kinetics of 4TU-labeled mRNAs is observed immediately upon addition of excess uracil in pulse–chase analyses. This does not appear to be the case when using wild-type strains of *S. cerevisiae* for similar metabolic labeling analyses. Studies using unlabeled uracil to chase [^{3}H]uracil in *S. cerevisiae* to measure mRNA half-lives indicate it takes several minutes for a >2000-fold excess of unlabeled uracil to effectively block the incorporation of [^{3}H]uracil into RNA (Crabeel *et al.* 1990). A study using 4TU to examine mRNA half-life uses a 10-min timepoint following the chase as the initial time point for determining half-life (Munchel *et al.* 2011) and the measured half-lives of *S. cerevisiae* mRNAs obtained by this procedure are longer than those determined from other methods. Explanations for this difference between these organisms might be that the addition of excess uracil does not immediately dilute the uracil or 4TU pool in *S. cerevisiae* because of differences in pyrimidine uptake, compartmentalization, or metabolism between *S. cerevisiae* and *N. crassa*.

The conceptual division between NMD-related processes in animals and plants and NMD-related processes in fungi because EJC-linked mRNA instability had not been previously demonstrated in the latter group is bridged by the work described here. Most work on fungal NMD has used *S. cerevisiae*, whose genome generally lacks introns. For this organism, it is logical to rationalize the absence of EJC-linked NMD because the dearth of introns in its genome could remove selective pressure to retain intron-processing linked quality-control mechanisms. However, the genomes of filamentous fungi are rife with introns and thus this quality-control mechanism would be expected to have important functions in *N. crassa* and other filamentous fungi. Our data indicate that there is a branch of NMD in *N. crassa* that corresponds to the faux-UTR branch in that there is no requirement for EJC or CBC factors but there is a requirement for at least UPF1 and UPF2. The stabilities of two uORF-containing mRNAs *arg-2* and *eif5* appear to be controlled by this branch, and it is likely that other uORF-containing or long 3′-UTR-containing mRNAs will be governed by this pathway.

Our data also demonstrate a second branch of NMD in which an intron downstream of a termination codon elicits NMD and requires EJC and CBC factors as well as at least UPF1 and UPF2. This second branch would have a role in quality control in destroying certain incorrectly or alternatively spliced mRNAs as well as governing levels of mRNAs that normally contain spliced 3′-UTR introns. Determining where there are differences between fungi and higher eukaryotes with respect to specific elements that comprise these mechanisms could provide targets for the development of new therapeutics; for example, the fungal pathogen *C. neoformans* is avirulent when it lacks XRN1, an exonuclease that has a central role in mRNA degradation (Wollschlaeger *et al.* 2014). The similarities between fungal systems and higher eukaryotes, and the experimental advantages that fungi offer, will enable experimental approaches for understanding the different branches of NMD and provide new opportunities for insights into fundamental mechanisms governing RNA stability.

Acknowledgments

We thank Meray Baştürkmen for initial development of the 4TU protocol, Cheng Wu for assistance with *in vitro* translation, and Allan Jacobson for helpful discussions. Strains were obtained from the Fungal Genetics Stock Center. This work was supported by National Institutes of Health R01 GM047498 and P01 GM068087. Neither Ying Zhang or Matthew S. Sachs has any financial conflict of interest that might be construed to influence the results or interpretation of this manuscript.

Literature Cited

Amrani, N., R. Ganesan, S. Kervestin, D. A. Mangus, S. Ghosh *et al.*, 2004 A faux 3′-UTR promotes aberrant termination and triggers nonsense-mediated mRNA decay. Nature 432: 112–118.

Amrani, N., M. S. Sachs, and A. Jacobson, 2006 Early nonsense: mRNA decay solves a translational problem. Nat. Rev. Mol. Cell Biol. 7: 415–425.

Bardiya, N., and P. K. Shiu, 2007 Cyclosporin A-resistance based gene placement system for *Neurospora crassa*. Fungal Genet. Biol. 44: 307–314.

Beelman, C. A., and R. Parker, 1994 Differential effects of translational inhibition in cis and in trans on the decay of the unstable yeast MFA2 mRNA. J. Biol. Chem. 269: 9687–9692.

Bicknell, A. A., C. Cenik, H. N. Chua, F. P. Roth, and M. J. Moore, 2012 Introns in UTRs: why we should stop ignoring them. BioEssays 34: 1025–1034.

Boswell, R. E., M. E. Prout, and J. C. Steichen, 1991 Mutations in a newly identified *Drosophila melanogaster* gene, mago nashi, disrupt germ cell formation and result in the formation of mirror-image symmetrical double abdomen embryos. Development 113: 373–384.

Buxton, F. P., and A. Radford, 1982 Partial characterization of 5-fluoropyrimidine-resistant mutants of *Neurospora crassa*. Mol. Gen. Genet. 185: 132–135.

Carter, M. S., J. Doskow, P. Morris, S. Li, R. P. Nhim *et al.*, 1995 A regulatory mechanism that detects premature nonsense codons in T-cell receptor transcripts in vivo is reversed by protein synthesis inhibitors in vitro. J. Biol. Chem. 270: 28995–29003.

Chan, W. K., L. Huang, J. P. Gudikote, Y. F. Chang, J. S. Imam *et al.*, 2007 An alternative branch of the nonsense-mediated decay pathway. EMBO J. 26: 1820–1830.

Cleary, M. D., C. D. Meiering, E. Jan, R. Guymon, and J. C. Boothroyd, 2005 Biosynthetic labeling of RNA with uracil phosphoribosyltransferase allows cell-specific microarray analysis of mRNA synthesis and decay. Nat. Biotechnol. 23: 232–237.

Colot, H. V., G. Park, G. E. Turner, C. Ringelberg, C. M. Crew *et al.*, 2006 A high-throughput gene knockout procedure for *Neurospora* reveals functions for multiple transcription factors. Proc. Natl. Acad. Sci. USA 103: 10352–10357.

Compton, J., 2003 p. 210 in *Advances in Understanding the Molecular Biology of Circadian Rhythms in Neurospora crassa*. University of California, Santa Cruz, CA.

Crabeel, M., R. LaValle, and N. Glansdorff, 1990 Arginine-specific repression in *Saccharomyces cerevisiae:* kinetic data on *ARG1* and *ARG3* mRNA transcription and stability support a transcriptional control mechanism. Mol. Cell. Biol. 10: 1226–1233.

Davis, R. H., and F. J. de Serres, 1970 Genetic and microbiological research techniques for *Neurospora crassa*. Methods Enzymol. 27A: 79–143.

Durand, S., and J. Lykke-Andersen, 2013 Nonsense-mediated mRNA decay occurs during eIF4F- dependent translation in human cells. Nat. Struct. Mol. Biol. 20: 702–709.

Dyer, B. W., F. A. Ferrer, D. K. Klinedinst, and R. Rodriguez, 2000 A noncommercial dual luciferase enzyme assay system for reporter gene analysis. Anal. Biochem. 282: 158–161.

Dzikiewicz-Krawczyk, A., P. Piontek, Z. Szweykowska-Kulinska, and A. Jarmolowski, 2008 The nuclear cap-binding protein complex is not essential for nonsense-mediated mRNA decay (NMD) in plants. Acta Biochim. Pol. 55: 825–828.

Ebbole, D., and M. S. Sachs, 1990 A rapid and simple method for isolation of *Neurospora crassa* homokaryons using microconidia. Fungal Genet. Newsl. 37: 17–18.

Feinberg, A. P., and B. Vogelstein, 1983 A technique for radiolabeling DNA restriction endonuclease fragments to high specific activity. Anal. Biochem. 132: 6–13.

Feldbrugge, M., K. Zarnack, E. Vollmeister, S. Baumann, J. Koepke *et al.*, 2008 The posttranscriptional machinery of *Ustilago maydis*. Fungal Genet. Biol. 45(Suppl. 1): S40–S46.

Gaba, A., A. Jacobson, and M. S. Sachs, 2005 Ribosome occupancy of the yeast *CPA1* upstream open reading frame termination codon modulates nonsense-mediated mRNA decay. Mol. Cell 20: 449–460.

Galagan, J. E., S. E. Calvo, C. Cuomo, L. J. Ma, J. R. Wortman *et al.*, 2005 Sequencing of *Aspergillus nidulans* and comparative analysis with *A. fumigatus* and *A. oryzae*. Nature 438: 1105–1115.

Ghosh, S., A. Obrdlik, V. Marchand, and A. Ephrussi, 2014 The EJC binding and dissociating activity of PYM is regulated in Drosophila. PLoS Genet. 10: e1004455.

Hachet, O., and A. Ephrussi, 2001 Drosophila Y14 shuttles to the posterior of the oocyte and is required for oskar mRNA transport. Curr. Biol. 11: 1666–1674.

Hachet, O., and A. Ephrussi, 2004 Splicing of oskar RNA in the nucleus is coupled to its cytoplasmic localization. Nature 428: 959–963.

Haimovich, G., D. A. Medina, S. Z. Causse, M. Garber, G. Millan-Zambrano *et al.*, 2013 Gene expression is circular: factors for mRNA degradation also foster mRNA synthesis. Cell 153: 1000–1011.

Herrick, D., R. Parker, and A. Jacobson, 1990 Identification and comparison of stable and unstable mRNAs in *Saccharomyces cerevisiae*. Mol. Cell. Biol. 10: 2269–2284.

Honda, S., and E. Selker, 2009 Tools for fungal proteomics: multifunctional Neurospora vectors for gene replacement, protein expression and protein purification. Genetics 182:11–23.

Hosoda, N., Y. K. Kim, F. Lejeune, and L. E. Maquat, 2005 CBP80 promotes interaction of Upf1 with Upf2 during nonsense-mediated mRNA decay in mammalian cells. Nat. Struct. Mol. Biol. 12: 893–901.

Hoyt, M. A., M. Broun, and R. H. Davis, 2000 Polyamine regulation of ornithine decarboxylase synthesis in *Neurospora crassa*. Mol. Cell. Biol. 20: 2760–2773.

Hsu, C. L., and A. Stevens, 1993 Yeast cells lacking 5′→3′ exoribonuclease 1 contain mRNA species that are poly(A) deficient and partially lack the 5′ cap structure. Mol. Cell. Biol. 13: 4826–4835.

Huang, L., C. H. Lou, W. Chan, E. Y. Shum, A. Shao *et al.*, 2011 RNA homeostasis governed by cell type-specific and branched feedback loops acting on NMD. Mol. Cell 43: 950–961.

Hwang, J., H. Sato, Y. Tang, D. Matsuda, and L. E. Maquat, 2010 UPF1 association with the capbinding protein, CBP80, promotes nonsense-mediated mRNA decay at two distinct steps. Mol. Cell 39: 396–409.

Ishigaki, Y., X. Li, G. Serin, and L. E. Maquat, 2001 Evidence for a pioneer round of mRNA translation: mRNAs subject to nonsense-mediated decay in mammalian cells are bound by CBP80 and CBP20. Cell 106: 607–617.

Isken, O., and L. E. Maquat, 2007 Quality control of eukaryotic mRNA: safeguarding cells from abnormal mRNA function. Genes Dev. 21: 1833–1856.

Karam, R., J. Wengrod, L. B. Gardner, and M. F. Wilkinson, 2013 Regulation of nonsense-mediated mRNA decay: implications for physiology and disease. Biochim. Biophys. Acta 1829: 624–633.

Kervestin, S., and A. Jacobson, 2012 NMD: a multifaceted response to premature translational termination. Nat. Rev. Mol. Cell Biol. 13: 700–712.

Kwon, Y. J., M. J. Park, S. G. Kim, I. T. Baldwin, and C. M. Park, 2014 Alternative splicing and nonsense-mediated decay of circadian clock genes under environmental stress conditions in Arabidopsis. BMC Plant Biol. 14: 136.

Lee, H. C., S. S. Chang, S. Choudhary, A. P. Aalto, M. Maiti *et al.*, 2009 qiRNA is a new type of small interfering RNA induced by DNA damage. Nature 459: 274–277.

Longman, D., N. Hug, M. Keith, C. Anastasaki, E. E. Patton *et al.*, 2013 DHX34 and NBAS form part of an autoregulatory NMD circuit that regulates endogenous RNA targets in human cells, zebrafish and *Caenorhabditis elegans*. Nucleic Acids Res. 41: 8319–8331.

Loughran, G., M. S. Sachs, J. F. Atkins, and I. P. Ivanov, 2012 Stringency of start codon selection modulates autoregu-

lation of translation initiation factor eIF5. Nucleic Acids Res. 40: 2898–2906.
Luo, Z., M. Freitag, and M. S. Sachs, 1995 Translational regulation in response to changes in amino acid availability in *Neurospora crassa*. Mol. Cell. Biol. 15: 5235–5245.
Maquat, L. E., W. Y. Tarn, and O. Isken, 2010 The pioneer round of translation: features and functions. Cell 142: 368–374.
Margolin, B. S., M. Freitag, and E. U. Selker, 1997 Improved plasmids for gene targeting at the *his-3* locus of *Neurospora crassa* by electroporation. Fungal Genet. Newsl. 44: 34–36.
McCluskey, K., A. Wiest, and M. Plamann, 2010 The Fungal Genetics Stock Center: a repository for 50 years of fungal genetics research. J. Biosci. 35: 119–126.
Mohr, S. E., S. T. Dillon, and R. E. Boswell, 2001 The RNA-binding protein Tsunagi interacts with Mago Nashi to establish polarity and localize oskar mRNA during Drosophila oogenesis. Genes Dev. 15: 2886–2899.
Morgan, L. W., and J. F. Feldman, 1997 Isolation and characterization of a temperature-sensitive circadian clock mutant of *Neurospora crassa*. Genetics 146: 525–530.
Morozov, I. Y., M. G. Jones, P. D. Gould, V. Crome, J. B. Wilson *et al.*, 2012 mRNA 3′ tagging is induced by nonsense-mediated decay and promotes ribosome dissociation. Mol. Cell. Biol. 32: 2585–2595.
Morozov, I. Y., S. Negrete-Urtasun, J. Tilburn, C. A. Jansen, M. X. Caddick *et al.*, 2006 Nonsense-mediated mRNA decay mutation in *Aspergillus nidulans*. Eukaryot. Cell 5: 1838–1846.
Munchel, S. E., R. K. Shultzaberger, N. Takizawa, and K. Weis, 2011 Dynamic profiling of mRNA turnover reveals gene-specific and system-wide regulation of mRNA decay. Mol. Biol. Cell 22: 2787–2795.
Nagarajan, V. K., C. I. Jones, S. F. Newbury, and P. J. Green, 2013 XRN 5′→3′ exoribonucleases: structure, mechanisms and functions. Biochim. Biophys. Acta 1829: 590–603.
Nicholson, P., H. Yepiskoposyan, S. Metze, R. Zamudio Orozco, N. Kleinschmidt *et al.*, 2009 Nonsense-mediated mRNA decay in human cells: mechanistic insights, functions beyond quality control and the double-life of NMD factors. Cell. Mol. Life Sci. 67: 677–700.
Nyiko, T., F. Kerenyi, L. Szabadkai, A. H. Benkovics, P. Major *et al.*, 2013 Plant nonsense-mediated mRNA decay is controlled by different autoregulatory circuits and can be induced by an EJC-like complex. Nucleic Acids Res. 41: 6715–6728.
Palacios, I. M., D. Gatfield, D. St Johnston, and E. Izaurralde, 2004 An eIF4AIII-containing complex required for mRNA localization and nonsense-mediated mRNA decay. Nature 427: 753–757.
Pall, M. L., and J. P. Brunelli, 1993 A series of six compact fungal transformation vectors containing polylinkers with multiple unique restriction sites. Fungal Genet. Newsl. 40: 58.
Popp, M. W., and L. E. Maquat, 2013 Organizing principles of mammalian nonsense-mediated mRNA decay. Annu. Rev. Genet. 47: 139–165.
Popp, M. W., and L. E. Maquat, 2014 The dharma of nonsense-mediated mRNA decay in mammalian cells. Mol. Cells 37: 1–8.
Pratt, R. J., and R. Aramayo, 2002 Improving the efficiency of gene replacements in *Neurospora crassa:* a first step towards a large-scale functional genomics project. Fungal Genet. Biol. 37: 56–71.
Rebbapragada, I., and J. Lykke-Andersen, 2009 Execution of nonsense-mediated mRNA decay: What defines a substrate? Curr. Opin. Cell Biol. 21: 394–402.
Ruepp, A., A. Zollner, D. Maier, K. Albermann, J. Hani *et al.*, 2004 The FunCat, a functional annotation scheme for systematic classification of proteins from whole genomes. Nucleic Acids Res. 32: 5539–5545.
Rufener, S. C., and O. Muhlemann, 2013 eIF4E-bound mRNPs are substrates for nonsense-mediated mRNA decay in mammalian cells. Nat. Struct. Mol. Biol. 20: 710–717.
Sachs, M. S., and C. Yanofsky, 1991 Developmental expression of genes involved in conidiation and amino acid biosynthesis in *Neurospora crassa*. Dev. Biol. 148: 117–128.
Saul, H., E. Elharrar, R. Gaash, D. Eliaz, M. Valenci *et al.*, 2009 The upstream open reading frame of the Arabidopsis AtMHX gene has a strong impact on transcript accumulation through the nonsense-mediated mRNA decay pathway. Plant J. 60: 1031–1042.
Sauliere, J., N. Haque, S. Harms, I. Barbosa, M. Blanchette *et al.*, 2010 The exon junction complex differentially marks spliced junctions. Nat. Struct. Mol. Biol. 17: 1269–1271.
Shi, C., I. T. Baldwin, and J. Wu, 2012 Arabidopsis plants having defects in nonsense-mediated mRNA decay factors UPF1, UPF2, and UPF3 show photoperiod-dependent phenotypes in development and stress responses. J. Integr. Plant Biol. 54: 99–114.
Stajich, J. E., T. Harris, B. P. Brunk, J. Brestelli, S. Fischer *et al.*, 2012 FungiDB: an integrated functional genomics database for fungi. Nucleic Acids Res. 40: D675–D681.
Sun, M., B. Schwalb, D. Schulz, N. Pirkl, S. Etzold *et al.*, 2012 Comparative dynamic transcriptome analysis (cDTA) reveals mutual feedback between mRNA synthesis and degradation. Genome Res. 22: 1350–1359.
Trcek, T., D. R. Larson, A. Moldon, C. C. Query, and R. H. Singer, 2011 Single-molecule mRNA decay measurements reveal promoter- regulated mRNA stability in yeast. Cell 147: 1484–1497.
Vogel, H. J., 1956 A convenient growth medium for *Neurospora* (Medium N). Microbiol. Genet. Bull. 13: 42–43.
Wei, J., C. Wu, and M. S. Sachs, 2012 The arginine attenuator peptide interferes with the ribosome peptidyl transferase center. Mol. Cell. Biol. 32: 2396–2406.
Wei, J., Y. Zhang, I. P. Ivanov, and M. S. Sachs, 2013 The stringency of start codon selection in the filamentous fungus *Neurospora crassa*. J. Biol. Chem. 288: 9549–9562.
Wen, J., and S. Brogna, 2010 Splicing-dependent NMD does not require the EJC in *Schizosaccharomyces pombe*. EMBO J. 29: 1537–1551.
Westergaard, M., and H. K. Mitchell, 1947 Neurospora V: a synthetic medium favoring sexual reproduction. Am. J. Bot. 34: 573–577.
Wollschlaeger, C., N. Trevijano-Contador, X. Wang, M. Legrand, O. Zaragoza *et al.*, 2014 Distinct and redundant roles of exonucleases in *Cryptococcus neoformans:* implications for virulence and mating. Fungal Genet. Biol. 73: 20–28.
Wu, C., N. Amrani, A. Jacobson, and M. S. Sachs, 2007 The use of fungal in vitro systems for studying translational regulation, pp. 203–225 in *Translation Initiation: Extract Systems and Molecular Genetics*, edited by J. Lorsch. Elsevier, San Diego.
Wu, C., Y. S. Kim, K. M. Smith, W. Li, H. M. Hood *et al.*, 2009 Characterization of chromosome ends in the filamentous fungus *Neurospora crassa*. Genetics 181: 1129–1145.
Wu, C., F. Yang, K. M. Smith, M. Peterson, R. Dekhang *et al.*, 2014 Genome-wide characterization of light-regulated genes in *Neurospora crassa*. G3 (Bethesda) 4: 1731–1745.
Yepiskoposyan, H., F. Aeschimann, D. Nilsson, M. Okoniewski, and O. Muhlemann, 2011 Autoregulation of the nonsense-mediated mRNA decay pathway in human cells. RNA 17: 2108–2118.
Zhang, S., E. M. Welch, K. Hogan, A. H. Brown, S. W. Peltz *et al.*, 1997 Polysome-associated mRNAs are substrates for the nonsense-mediated mRNA decay pathway in *Saccharomyces cerevisiae*. RNA 3: 234–244.
Zid, B. M., and E. K. O'Shea, 2014 Promoter sequences direct cytoplasmic localization and translation of mRNAs during starvation in yeast. Nature 514: 117–121.

Communicating editor: M. Freitag

GENETICS

Supporting Information
http://www.genetics.org/lookup/suppl/doi:10.1534/genetics.115.176743/-/DC1

Control of mRNA Stability in Fungi by NMD, EJC and CBC Factors Through 3′UTR Introns

Ying Zhang and Matthew S. Sachs

DOI: 10.1534/genetics.115.176743

Supplemental Information: Control of mRNA stability in fungi by NMD, EJC and CBC factors through 3'UTR introns

Ying Zhang and Matthew S. Sachs

Supplemental Tables

Table S1 Homologs of NMD, EJC, CBC factors and other components related to these pathways.

The *N. crassa* homologs identified represent the best bidirectional hits for each organism as determined using BLASTP at the NCBI website.

Exceptions are indicated.

Protein Name	Organism	NCBI Reference Sequence[a]	Reciprocal BLAST[b]	Ref/Note
Upf1	*N. crassa*	XP_961233.1		NCU04242
	S. pombe	NP_593080.1	XP_961233.1	Upf1
	S. cerevisiae	NP_013797.1	XP_961233.1	NAM7
	H. sapiens	NP_001284478.1	XP_961233.1	regulator of nonsense transcripts 1 isoform 1
	C. elegans	NP_490829.1	XP_961233.1	SMG-2
Upf2	*N. crassa*	XP_961757.2		NCU05267
	S. pombe	NP_593784.1	XP_961757.2	Upf2
	S. cerevisiae	NP_011944.2	XP_961757.2	Nmd2p
	H. sapiens	NP_056357.1	XP_961757.2	regulator of nonsense transcripts 2
	C. elegans	NP_500974.2	XP_961757.2	SMG-3
Upf3	*N. crassa*	XP_956721.1		NCU03435
	S. cerevisiae	NP_011586.1	XP_956721.1	Upf3p
	H. sapiens	NP_075386.1	XP_956721.1	regulator of nonsense transcripts 3B isoform 2
	C. elegans	(NP_741600.1)[c]	XP_956721.1	SMG-4, isoform b
Xrn1	*N. crassa*	XP_960925.2		NCU06678
	S. pombe	NP_593482.1	XP_960925.2	exonuclease II Exo2
	S. cerevisiae	NP_011342.1	XP_960925.2	Xrn1p
	H. sapiens	NP_001269786.1	XP_960925.2	5'-3' exoribonuclease 1 isoform c
	C. elegans	NP_496945.3	XP_960925.2	XRN-1
Y14	*N. crassa*	XP_965326.1		NCU03226
	S. pombe	NP_594439.1	XP_965326.1	
	S. cerevisiae	not detected		
	H. sapiens	NP_005096.1	XP_965326.1	
	C. elegans	NP_497891.1	XP_965326.1	RNP-4
	X. laevis	NP_001079905.1	XP_965326.1	RNA-binding protein 8A-B

	D. melanogaster	NP_610454.2	XP_965326.1	tsunagi
	A. thaliana	NP_564591.1	XP_965326.1	
Mago	*N. crassa*	XP_957482.1		NCU04405
	S. pombe	NP_596666.1	XP_957482.1	mago nashi
	S. cerevisiae	not detected		
	H. sapiens	NP_060518.1	XP_957482.1	mago nashi
	C. elegans	NP_493025.1	XP_957482.1	MAG-1
	X. laevis	NP_001079724.1	XP_957482.1	mago nashi
	D. melanogaster	NP_476636.1	XP_957482.1	mago nashi
	A.thaliana	NP_171716.1	XP_957482.1	mago nashi
eIF4AIII	*N. crassa*	XP_961600.1		NCU01234
	S. pombe	NP_592863.1	XP_961600.1	
	S. cerevisiae	NP_010304.3	XP_961600.1	FAL1
	H. sapiens	NP_055555.1	XP_961600.1	eIF4AIII
	C. elegans	NP_490761.2	XP_961600.1	
	X. laevis	NP_001084200.1	XP_961600.1	eIF4A-III-B
	D. melanogaster	NP_649788.2	XP_961600.1	eIF4AIII
	A.thaliana	NP_188610.1	XP_961600.1	DEAD-box ATP-dependent RNA helicase 2
Btz[d]				
RNPS1	*N. crassa*	XP_958016.1		NCU09901
	S. pombe	NP_596549.2	XP_958016.1	RNA-binding protein (predicted)
	S. cerevisiae	NP_015147.1[e]	XP_956595.1	Cbc2p
	H. sapiens	NP_001273556.1	XP_958016.1	RNA-binding protein with serine-rich domain 1 isoform c
	C. elegans	NP_497276.2	XP_958016.1	Protein RNP-5
CBP20	*N. crassa*	XP_956595.1		NCU00210
	S. pombe	NP_596414.1	XP_956595.1	nuclear cap-binding complex small subunit (predicted)
	S. cerevisiae	NP_015147.1	XP_956595.1	Cbc2p
	H. sapiens	NP_031388.2	XP_956595.1	nuclear cap-binding protein subunit 2 isoform 1
	C. elegans	NP_001250552.1	XP_956595.1	NCBP-2, isoform a
CBP80	*N. crassa*	XP_961147.1		NCU04187
	S. pombe	NP_594104.1	XP_961147.1	nuclear cap-binding complex large subunit (predicted)
	S. cerevisiae	NP_013844.2	XP_961147.1	Sto1p
	H. sapiens	NP_002477.1	XP_961147.1	nuclear cap-binding protein subunit 1
	C. elegans	NP_491850.2	XP_961147.1	NCBP-1
eRF1	*N. crassa*	XP_957296.1		NCU00410
	S. pombe	NP_594680.1	XP_957296.1	eRF1
	S. cerevisiae	NP_009701.3	XP_957296.1	eRF1
	H. sapiens	NP_004721.1	XP_957296.1	eukaryotic peptide chain release factor subunit 1 isoform 1
	C. elegans	NP_001024107.2	XP_957296.1	ETF-1

eIF4A[f]	*N. crassa*	XP_958421.2		NCU07420
	S. pombe	NP_594854.1	XP_958421.2	eIF4A
	S. cerevisiae	NP_012397.1	XP_958421.2	eIF4A
	H. sapiens	NP_001407.1	XP_958421.2	eIF4A-I isoform 1
	C. elegans	NP_001022623.1	XP_958421.2	INF-1, isoform a

[a]. The N. crassa protein was used in BLAST and the entry represents the top hit

[b]. The top hit identified in each organism was used to BLAST N. crassa proteins and the entry represents the top hit to evaluate best bidirectional hits

[c]. N. crassa Upf3 did not give a significant hit when BLASTed against C. elegans, but C. elegans SMG4 identifies N. crassa NCU03435

[d]. No Btz homolog was identified in N. crassa

[e]. The protein identified as N. crassa RNPS1 has a best hit to S. cerevisiae CBP20 (which reciprocally hits N. crassa CBP20)

[f]. eIF4A is distinct from eIF4AIII and the homologs are included here for reference

Table S2 Phenotypes of selected *N. crassa* deletion strains.

Phenotypes of the wild-type strain (wt), and indicated mutant strains were assessed as described in Materials and Methods.

FGSC #	Genotype	Gene Name	Colony Growth and Morphology (Growth Pattern)				Colony Growth and Morphology (Plate Pigmentation)				25°C Growth in Slant Cultures			25°C Growth Rate of Basal Hyphae (mm/hr)	25°C Aerial Hyphae Height (mm/day)		Female Sexual Development		
			VM		VM+YE		VM		VM+YE		Slant Pigmen-tation	Conid-iation	Aerial Hyphae Forma-tion		VM	VM +YE	Protoper-ithecium Forma-tion	Perithe-cium Forma-tion	Asco-spore Forma-tion
			25	37	25	37	25	37	25	37									
2489	wild-type		+	+	+	+	+	+	+	+	+	+	+	2.8	20-25	20-25	+	+	+
11230	ΔNCU04242	upf1	-	-	-	+	r	r	r	r	r	r	r	2.2	15-20	15-20	+	+	+
15706	ΔNCU05267	upf2	-	-	-	-	r	r	r	r	r	r	short	2	5-10	10-15	r	-	-
11679	ΔNCU03435	upf3	+	+	+	+	+	+	+	+	r	r	r	2.9	20-25	15-20	+	+	+
13031	ΔNCU04405	mago	-	+	-	+	r	r	r	r	r	+	r	1.7	15-20	15-20	-	-	-
15492	ΔNCU03226	y14	-	-	-	-	r	r	r	r	r	r	+	0.4	0-5	0-5	-	-	-
19228	ΔNCU06678	xrn1	-	-	-	-	+	r	+	r	+	r	r	1.6	10-15	10-15	+	+	r
17986	ΔNCU04270	btz	+	+	+	+	+	+	+	+	+	+	+	2.9	20-25	20-25	r	+	r
12342	ΔNCU09901	rnps1	+	+	+	+	+	+	+	+	+	+	+	3	20-25	25-30	+	+	+
18692	ΔNCU00210	cbp20	+	+	+	+	-	-	-	+	+	+	+	2.2	20-25	20-25	+	+	+
22440	ΔNCU04187	cbp80	+	+	-	+	+	+	+	+	+	+	+	2.8	20-25	20-25	+	+	+
20906	ΔNCU05889	eif3e	-	-	-	-	-	-	-	-	r	-	-	0.8	5-10	0-5	-	-	-

"+" : normal
"-" : not formed
"r" : reduced formation

Table S3 Identified *N. crassa* transcripts with at least one spliced 3'UTR intron.

The *Neurospora crassa* gene models from release 7 indicates 321 of the 9728 predicted protein coding genes in *N. crassa* potentially have 3'UTR introns. For 237, the 3'UTR-intron was present in all expected forms of the transcript were further examined according to our recently published RNA-seq data for wt (Wu *et al.* 2014). 31 mRNAs with spliced 3'UTR introns were identified and their predicted 3'UTR and 3'UTR intron-lengths were calculated based on *N. crassa* RNA-seq data; additional information about these genes is also listed.

Locus	Predicted 3'UTR Left [intron] Right	Gene Symbol or Description	Protein
NCU00261	471 [64] 327	pyr-7	CTP synthase
NCU00410	235 [55] 366	erf1	eukaryotic release factor 1
NCU00778	53 [57] 412	sed5 vesicle protein	sed5 vesicle protein
NCU00854	131 [58] 21	hypothetical protein	hypothetical protein
NCU01234	139 [62] 93 or 180	eif4a3	eukaryotic initiation factor 4A-12
NCU01312	102 [62] 380	rca-1	regulator of conidiation in Aspergillus-1
NCU01888	98 [69] 321	tRNA-specific adenosine deaminase	tRNA-specific adenosine deaminase
NCU01907	92 [68] 148	syntaxin 5	syntaxin 5
NCU02174	9 [170] 501	hypothetical protein	hypothetical protein
NCU02249	337 [63] 784	hat-5	histone acetyltransferase
NCU02423	36 [93] 880	mic-12	mitoferrin-1
NCU02885	104 [63] 1253	stk-20	hypothetical protein
NCU02948	12 [78] 277	ncw-4	non-anchored cell wall protein-4
NCU03226	394 [60] 375	y14	Y14 protein
NCU03491	43 [56] 704	pad-1	Paddle-1
NCU03682	184 [71] 250	endonuclease/exonuclease/phosphatase	endonuclease/exonuclease/phosphatase
NCU04650	194 [75] 562	hypothetical protein	hypothetical protein
NCU04699	104 [63] 599	chol-2	methylene-fatty-acyl-phospholipid synthase
NCU04986	131 [60] 71	hypothetical protein	hypothetical protein
NCU05243	14 [69] 174	hypothetical protein	hypothetical protein
NCU05964	69 [65] 741	developmental regulator VosA	developmental regulator VosA
NCU06322	359 [131] 231	drc-2/DNA replication complex GINS protein psf-2	DNA replication complex GINS protein psf-2
NCU06869	541 [55] 436	paa-9	cleavage and polyadenylylation specificity factor
NCU07408	220 [215] 109	po	60S ribosomal protein P0
NCU07587	382 [60] 182	div-16/Swi6	Swi6
NCU08026	71 [63] 697	3' exoribonuclease	3' exoribonuclease
NCU08727	289 [59] 261	hypothetical protein	hypothetical protein
NCU09615	197 [60] 345	hypothetical protein	hypothetical protein
NCU10500	118 [77] 492	F-box domain-containing protein	F-box domain-containing protein
NCU10572	70 [75] 484	short chain oxidoreductase	short chain oxidoreductase
NCU11426	535 [107] 342	nuc-2	nuc-2 protein

Table S4 FunCat analysis for identified *N. crassa* transcripts with at least one spliced 3'UTR intron.

The FunCat database (Ruepp *et al.* 2004) was used to calculate functional enrichments for the products specified by the 31 identified mRNAs with spliced 3'UTR introns as described in Materials and Methods.

FUNCTIONAL CATEGORY	abs SET	rel SET	genes SET	abs GENOME	rel GENOME	rel SET/rel GENOME	P-VALUE
01.03 nucleotide/nucleoside/nucleobase metabolism	8	28.5	NCU00261 NCU02423 NCU01234 NCU11426 NCU01888 NCU07408 NCU08026 NCU03226	745	7.4	3.851	0.001
01.03.04 pyrimidine nucleotide/nucleoside/nucleobase metabolism	3	10.7	NCU00261 NCU11426 NCU01888	159	1.57	6.815	0.009
01.03.04.01 pyrimidine nucleotide/nucleoside/nucleobase catabolism	2	7.14	NCU11426 NCU01888	29	0.28	25.500	0.003
01.03.16 polynucleotide degradation	5	17.8	NCU01234 NCU11426 NCU07408 NCU08026 NCU03226	220	2.18	8.165	0.000
01.03.16.01 RNA degradation	4	14.2	NCU01234 NCU07408 NCU08026 NCU03226	153	1.51	9.404	0.001
01.06.02 membrane lipid metabolism	3	10.7	NCU00261 NCU04699 NCU11426	262	2.6	4.115	0.035
01.06.02.01 phospholipid metabolism	3	10.7	NCU00261 NCU04699 NCU11426	189	1.87	5.722	0.015
10 CELL CYCLE AND DNA PROCESSING	9	32.1	NCU02249 NCU01312 NCU01234 NCU04650 NCU11426 NCU06322 NCU07587 NCU02885 NCU03226	1715	17	1.888	0.038
10.01 DNA processing	8	28.5	NCU02249 NCU01312 NCU01234 NCU11426 NCU06322 NCU07587 NCU02885 NCU03226	1117	11	2.591	0.009
10.01.03 DNA synthesis and replication	4	14.2	NCU02249 NCU01234 NCU06322 NCU07587	365	3.62	3.923	0.017
10.01.05 DNA recombination and DNA repair	5	17.8	NCU02249 NCU01234 NCU11426 NCU07587 NCU02885	558	5.54	3.213	0.017
10.01.05.01 DNA repair	4	14.2	NCU02249 NCU01234 NCU11426 NCU02885	477	4.73	3.002	0.041
10.03.01.01.03 G1/S transition of mitotic cell cycle	3	10.7	NCU01312 NCU07587 NCU02885	159	1.57	6.815	0.009
10.03.04 nuclear and chromosomal cycle	3	10.7	NCU04650 NCU11426 NCU02885	289	2.87	3.728	0.045
11 TRANSCRIPTION	15	53.5	NCU02249 NCU02423 NCU01312 NCU01234 NCU04986 NCU11426 NCU01888 NCU06869 NCU07408 NCU07587 NCU08026 NCU02948 NCU02885 NCU09615 NCU03226	1759	17.4	3.075	0.000
11.02 RNA synthesis	10	35.7	NCU02249 NCU01312 NCU01234 NCU04986 NCU11426 NCU06869 NCU07587 NCU02948 NCU09615 NCU03226	1489	14.7	2.429	0.005
11.02.03 mRNA synthesis	10	35.7	NCU02249 NCU01312 NCU01234 NCU04986 NCU11426 NCU06869 NCU07587 NCU02948 NCU09615 NCU03226	1426	14.1	2.532	0.004
11.02.03.04 transcriptional control	9	32.1	NCU02249 NCU01312 NCU01234 NCU11426 NCU06869 NCU07587 NCU02948 NCU09615 NCU03226	1279	12.7	2.528	0.006

11.04 RNA processing	9	32.1	NCU02423 NCU01312 NCU01234 NCU11426 NCU06869 NCU07408 NCU08026 NCU02885 NCU03226	732	7.27	4.415	0.000
11.04.01 rRNA processing	4	14.2	NCU01234 NCU07408 NCU08026 NCU03226	363	3.6	3.944	0.017
11.04.03 mRNA processing (splicing, 5^-, 3^-end processing)	9	32.1	NCU02423 NCU01312 NCU01234 NCU11426 NCU06869 NCU07408 NCU08026 NCU02885 NCU03226	538	5.34	6.011	0.000
11.04.03.01 splicing	5	17.8	NCU02423 NCU01312 NCU01234 NCU06869 NCU03226	437	4.34	4.101	0.006
11.04.03.05 3^-end processing	2	7.14	NCU06869 NCU03226	84	0.83	8.602	0.023
11.04.03.11 control of mRNA stability	3	10.7	NCU01234 NCU02885 NCU03226	95	0.94	11.383	0.002
12 PROTEIN SYNTHESIS	6	21.4	NCU00410 NCU01234 NCU07408 NCU08026 NCU02885 NCU03226	753	7.47	2.865	0.016
12.04 translation	4	14.2	NCU00410 NCU01234 NCU07408 NCU03226	460	4.56	3.114	0.037
16 PROTEIN WITH BINDING FUNCTION OR COFACTOR REQUIREMENT (structural or catalytic)	17	60.7	NCU00410 NCU02249 NCU02423 NCU01312 NCU01234 NCU00778 NCU04650 NCU11426 NCU06322 NCU01888 NCU01907 NCU06869 NCU07408 NCU07587 NCU08026 NCU02885 NCU03226	3639	36.1	1.681	0.007
16.01 protein binding	13	46.4	NCU00410 NCU02249 NCU01312 NCU01234 NCU00778 NCU04650 NCU11426 NCU01907 NCU06869 NCU07408 NCU07587 NCU02885 NCU03226	2333	23.1	2.009	0.006
16.03 nucleic acid binding	10	35.7	NCU02249 NCU01312 NCU01234 NCU04650 NCU11426 NCU06322 NCU06869 NCU07587 NCU08026 NCU03226	1290	12.8	2.789	0.002
16.03.01 DNA binding	7	25	NCU02249 NCU01312 NCU01234 NCU11426 NCU06322 NCU07587 NCU03226	854	8.48	2.948	0.007
16.03.03 RNA binding	6	21.4	NCU01234 NCU04650 NCU11426 NCU06869 NCU08026 NCU03226	552	5.48	3.905	0.004
16.07 structural protein binding	2	7.14	NCU04650 NCU07408	94	0.93	7.677	0.028
18.02.01.01 enzyme activator	4	14.2	NCU00410 NCU11426 NCU06869 NCU02885	376	3.73	3.807	0.019
18.02.01.02.05 kinase inhibitior	2	7.14	NCU11426 NCU02885	103	1.02	7.000	0.033
20 CELLULAR TRANSPORT, TRANSPORT FACILITIES AND TRANSPORT ROUTES	11	39.2	NCU02423 NCU01312 NCU01234 NCU00778 NCU04650 NCU11426 NCU01907 NCU07587 NCU08026 NCU02948 NCU02885	2165	21.5	1.823	0.025
20.01.13 lipid/fatty acid transport	3	10.7	NCU02423 NCU11426 NCU07587	206	2.04	5.245	0.019
20.09 transport routes	8	28.5	NCU02423 NCU01234 NCU00778 NCU04650 NCU11426 NCU01907 NCU07587 NCU02885	1454	14.4	1.979	0.040
20.09.07 vesicular transport (Golgi network, etc.)	6	21.4	NCU00778 NCU04650 NCU11426 NCU01907 NCU07587 NCU02885	521	5.17	4.139	0.003
20.09.07.05 intra Golgi transport	2	7.14	NCU00778 NCU01907	74	0.73	9.781	0.018
30.01.09.03 Ca2+ mediated signal transduction	2	7.14	NCU11426 NCU02885	125	1.24	5.758	0.047
32.01.06 cold shock response	2	7.14	NCU01234 NCU11426	65	0.64	11.156	0.014

34.11.09 temperature perception and response	2	7.14	NCU02423 NCU11426	110	1.09	6.550	0.037
42.04.03 actin cytoskeleton	3	10.7	NCU11426 NCU07587 NCU02885	275	2.73	3.919	0.040

[a]The comparison is done to p3_p13841_Neu_crass_MIPS containing 10067 annotated genes.
28 out of 31 genes are found:
NCU00261 NCU00410 NCU00778 NCU00854 NCU01234 NCU01312 NCU01888 NCU01907 NCU02174 NCU02249 NCU02423 NCU02885 NCU02948 NCU03226 NCU03682 NCU04650 NCU04699 NCU04986 NCU05243 NCU05964 NCU06322 NCU06869 NCU07408 NCU07587 NCU08026 NCU08727 NCU09615 NCU11426

Table S5 *N. crassa* strains used in this study.

Strain	Genotype	Reference
FGSC2489	*mat A (74-OR23-1VA)*	FGSC
FGSC4200	*mat a (ORS-SL6a)*	FGSC
FGSC6103	*mat A, his-3*$^{-}$	FGSC
RANCR6A	*mat a, his-3, inl*	(Pratt and Aramayo 2002)
FGSC16561	*mat a, Δuc-4(NCU01446) ::hph*	(Colot *et al.* 2006)
FGSC11230	*mat A, Δupf1::hph*	(Colot *et al.* 2006)
FGSC15706	*mat a, Δupf2::hph*	(Colot *et al.* 2006)
FGSC11679	*mat a, Δupf3::hph*	(Colot *et al.* 2006)
FGSC19228	*mat a, Δxrn1::hph*	(Colot *et al.* 2006)
FGSC15492	*mat a, Δy14::hph*	(Colot *et al.* 2006)
FGSC13031	*mat A, Δmago::hph*	(Colot *et al.* 2006)
FGSC22440	*mat A, Δcbp80::hph*	(Colot *et al.* 2006)
FGSC18692	*mat a, Δcbp20::hph*	(Colot *et al.* 2006)
NZ060	*mat A, his-3+::upf1*$_P$*-upf1, Δupf1::hph*	microconidiation
NZ070	*mat A, his-3+::upf1*$_P$*-upf1-Gly-3xFLAG, Δupf1::hph*	microconidiation
NZ100	*mat a, his-3+::upf2*$_P$*-upf2-Gly3xFLAG, Δupf2::hph*	microconidiation
NZ110	*mat a, his-3+::upf2*$_P$*-upf2-GlyHATFLAG, Δupf2::hph*	microconidiation
NZ130	*mat a, y14*$_P$*-y14-Bar, Δy14::hph*	microconidiation
NZ140	*mat A, mago*$_P$*-mago-Bar, Δmago::hph*	microconidiation
NZ150	*mat a, xrn1*$_P$*-xrn1-Bar, Δxrn1::hph*	microconidiation
NZ160	*mat A, cbp80*$_P$*-cbp80-Bar, Δcbp80::hph*	microconidiation
NZ170	*mat a, cbp20-cbp20-Bar, Δcbp20::hph*	microconidiation
Luciferase reporter strains		
NZ1000	*mat A; his-3+::cox-5*$_P$*|cox-5|luc|cox-5*	microconidiation
NZ1001	*mat A; his-3+::cox-5*$_P$*|cox-5|luc|cox-5; Δupf1:: hph*	microconidiation
NZ1005	*mat A; his-3+::cox-5*$_P$*|cox-5|luc|eIF4A3+i*	microconidiation
NZ1006	*mat A; his-3+::cox-5*$_P$*|cox-5|luc|eIF4A3+i; Δupf1:: hph*	microconidiation
NZ1011	*mat A; his-3+::cox-5*$_P$*|cox-5|luc|eIF4A3-i*	microconidiation
NZ1012	*mat A; his-3+::cox-5*$_P$*|cox-5|luc|eIF4A3-i; Δupf1:: hph*	microconidiation
NZ1017	*mat A; his-3+::cox-5*$_P$*|AAP|luc|cox-5*	cross
NZ1018	*mat A; his-3+::cox-5*$_P$*|AAP|luc|cox-5; Δupf1:: hph*	cross
NZ1021	*mat a; his-3+::cox-5*$_P$*::AAP*$_{D12N}$*::Luc::cox-5*	cross
NZ1030	*mat A; his-3+::cox-5*$_P$*::AAP*$_{D12N}$*::Luc::cox-5; Δupf1:: hph*	cross
NZ1031	*mat A; csr-1::cox-5*$_P$*|cox-5|luc|cox-5*	cross
NZ1036	*mat a; csr-1::cox-5*$_P$*|cox-5|luc|cox-5; Δy14:: hph*	cross
NZ1037	*mat A; csr-1::cox-5*$_P$*|cox-5|luc|eIF4A3+i*	cross
NZ1040	*mat a csr-1::cox-5*$_P$*|cox-5|luc|eIF4A3+i; Δy14::hph*	cross
NZ1041	*mat A; csr-1::cox-5*$_P$*|cox-5|luc|eIF4A3-i*	cross
NZ1046	*mat a; csr-1::cox-5*$_P$*|cox-5|luc|eIF4A3-i; Δy14::hph*	cross
NZ1047	*mat A; his-3+::cox-5*$_P$*|cox-5|luc|eRF1+i*	cross
NZ1052	*mat A; his-3+::cox-5*$_P$*|cox-5|luc|eRF1+i; Δupf1:: hph*	cross
NZ1053	*mat A; his-3+::cox-5*$_P$*|cox-5|luc|eRF1-i*	cross
NZ1058	*mat A; his-3+::cox-5*$_P$*|cox-5|luc|eRF1-i; Δupf1:: hph*	cross
NZ1059	*mat A; csr-1::cox-5*$_P$*|cox-5|luc|cox-5; Δcbp80:: hph*	cross
NZ1062	*mat A csr-1::cox-5*$_P$*|cox-5|luc|eIF4A3+i; Δcbp80::hph*	cross
NZ1063	*mat A csr-1::cox-5*$_P$*|cox-5|luc|eIF4A3-i;Δcbp80::hph*	cross
NZ1065	*mat A; csr-1::cox-5*$_P$*|cox-5|luc|cox-5; Δcbp20:: hph*	cross
NZ1066	*mat A csr-1::cox-5*$_P$*|cox-5|luc|eIF4A3+i; Δcbp20::hph*	cross
NZ1067	*mat A csr-1::cox-5*$_P$*|cox-5|luc|eIF4A3-i; Δcbp20::hph*	cross
NZ1068	*mat A; csr-1::cox-5*$_P$*|cox-5|luc|cox-5; Δcbp20:: hph;Δcbp80:: hph*	cross
NZ1069	*mat A; csr-1::cox-5*$_P$*|cox-5|luc|eIF4A3+i; Δcbp20:: hph;Δcbp80:: hph*	cross
NZ1070	*mat A; csr-1::cox-5*$_P$*|cox-5|luc|eIF4A3-i; Δcbp20:: hph;Δcbp80:: hph*	cross

Table S6 Plasmids used for rescuing *N. crassa* deletion mutants.

Plasmid	Promoter-coding region	PCR oligo	Oligonucleotide sequence, 5′ → 3′	Cloning site	Vector
pZY05	his3::upf1$_P$-upf1	oYZ165	CTTGGCGGCCGCTTTCTAGAATACAG	NotI	pBM61
		oYZ166	CGGAATTCGACCGCCAGCTAACCCAAC	EcoRI	
pZY43	his3::upf1$_P$-upf1-Gly-3xFLAG	oYZ165	CTTGGCGGCCGCTTTCTAGAATACAG	NotI	pCCGC-Gly3xFLAG (FJ457001)
		oYZ194	CGTTAATTAAATCGAAACCTGTCCCGATCTGACTGGC	PacI	
pZY68	his3::upf2$_P$-upf2-Gly3xFLAG	oYZ219	GGGCGGCCGCAGCTCAAGGGAAGCCAAC	NotI	pCCGC-Gly3xFLAG (FJ457001)
		oYZ220	CCACTAGTACTGGGCGATGAGAATC	SpeI	
pZY70	his3::upf2$_P$-upf2-GlyHATFLAG	oYZ221	GGACTAGTGGATGGATCGCCAAAG	SpeI	pCCGC-GlyHATFLAG (FJ457003)
		oYZ222	GGTTAATTAAAGTCCAATCAACATCAC	PacI	
pZY125	xrn1$_P$-xrn1-[Bar^r]	oYZ477	GGGCATATGTGTTGTCTTTATTTAGAGCCG	NdeI	pBARGPE1 (DBP 357)
		oYZ478	CATACGCGTCATCAACTTCTCCCTCG	MluI	
pZY120	y14$_P$-y14-[Bar^r]	oYZ435	CTTCCATATGAACCGCAACGATTGC	NdeI	pBARGPE1 (DBP 357)
		oYZ436	GCTACGCGTTTTCGTCACAGCCTAC	MluI	
pZY104	mago$_P$-mago-[Bar^r]	oYZ437	CCTCATATGTACTCGTTCGGGTGTTG	NdeI	pBARGPE1 (DBP 357)
		oYZ438	GTTCACGCGTCAACAGTCAAGTTGTATC	MluI	
pZY128	cbp20$_P$-cbp20-[Bar^r]	oYZ501	GGCCATATGGAGGTCTTAACGGAGAC	NdeI	pBARGPE1 (DBP 357)
		oYZ502	GTTAAACGCGTCGTCGCCACCATTGAG	MluI	
pZY126	cbp80$_P$-cbp80-[Bar^r]	oYZ479	GGGCATATGATGGATTATGGCATATAGGG	NdeI	pBARGPE1 (DBP 357)
		oYZ481	CATACGCGTGGTGAAGGATGTTGG	MluI	

Table S7 Vectors and oligonucleotides used to construct luciferase reporters.

Plasmid	Description	Insert Oligo	Oligonucleotide sequence, 5′ → 3′	Cloning site	Vector(s)
pZY78	his-3::cox-5_P|cox-5|luc|	oYZ335	GCTCTAGAGTTACGCGTGCTTGTGATTGGAAG	XbaI	pRMP57
		oYZ336	CGACTAGTTACCGGTAGGAGTGAAGTCTTGCAAAG	SpeI	
pZY82	his-3::cox-5_P|cox-5|luc|cox-5	oYZ339	GCCATTAATTAAGTTTCGCATACTTTTATTGG	PacI	pZY78
		oYZ340	GCTTAATTAATGCAATAGATCACACGTC	PacI	
pZY118	his-3::cox-5_P|AAP|luc|cox-5	oYZ169	CTGGGATCCAACTTGTCTTGTCGC	BamHI	pZY82[2], pPR101[3]
		oYZ170	CGCCCGGGCTTGACTTGAATGGT	XmaI	
pZY119	his-3::cox-5_P|D12N|luc|cox-5	oYZ169	CTGGGATCCAACTTGTCTTGTCGC	BamHI	pZY82, D12N (pPS101)
		oYZ170	CGCCCGGGCTTGACTTGAATGGT	XmaI	
pZY92	his-3::cox-5_P|cox-5|luc|eIF4A3+I	oYZ330	TTATTAATTAAGAGGCTAGCGCGGGG	PacI	pZY78
		oYZ332	CCACTTAATTAACACCTGCGCGGG	PacI	
pZY94	his-3::cox-5_P|cox-5|luc|eIF4A3-I	oYZ330	TTATTAATTAAGAGGCTAGCGCGGGG	PacI. Overlapping PCR	pZY78
		oYZ334	CAATCTGTAAAGCGTCCTTAAGGCCGACATGC		
		oYZ333	GCATGTCGGCCTTAAGGACGCTTTACAGATTG		
		oYZ332	CCACTTAATTAACACCTGCGCGGG		
pZY84	his-3::cox-5_P|cox-5|luc|eRF1+I	oYZ181	GCCTTAATTAACAAGTTGAATCCCTCGCCG	PacI	pZY78
		oYZ329	CGCGTTAATTAATCTCATGAACACTACTGG	PacI	
pZY86	his-3::cox-5_P|cox-5|luc|eRF1-I	oYZ181	GCCTTAATTAACAAGTTGAATCCCTCGCCG	PacI	pZY78
		oYZ182	GGCCTTAATTAAACAAAGACAGAATGAGCG		
		oYZ329	CGCGTTAATTAATCTCATGAACACTACTGG	PacI	
pZY122	csr-1::cox-5_P|cox-5|luc|cox-5	NotI/ClaI fragment from pZY82		NotI	pCSR1
				ClaI	
pZY123	csr-1::cox-5_P|cox-5|luc|eIF4A3+I	NotI/ClaI fragment from pZY96		NotI	pCSR1
				ClaI	
pZY124	csr-1::cox-5_P|cox-5|luc|eIF4A3-I	NotI/ClaI fragment from pZY98		NotI	pCSR1
				ClaI	

Table S8 Oligonucleotide primers used for 3'RACE.

Oligonucleotide for 3'RACE			
PCR oligo			Oligonucleotide sequence, 5′ → 3′
3'–RACE CDS Primer A		oYZ291	AAGCAGTGGTATCAACGCAGAGTAC(T)30VN
Nested Universal Primer A		oYZ294	AAGCAGTGGTATCAACGCAGAGT
luc-cox-5	Nest oligo1	oYZ365	CGTCTTCGTCGACGAGGTCC
	Nest oligo2	oYZ287	GGCCAAGAAGGGCGGCAAGATCGCCGTC
luc-eIF4A3	Nest oligo1	oYZ365	CGTCTTCGTCGACGAGGTCC
	Nest oligo2	oYZ287	GGCCAAGAAGGGCGGCAAGATCGCCGTC
eIF4A3	Nest oligo1	oYZ027	CCCGCGGTATCGATGTTC
	Nest oligo2	oYZ330	CCCGCGGTATCGATGTTC
Oligonucleotide for 3´UTR intron (+/-) detection			
PCR oligo			Oligonucleotide sequence, 5′ → 3′
eIF4A3 (411/349)	oYZ330		TTATTAATTAAGAGGCTAGCGCGGGG
	oYZ482		GCGAAATAAACCCCGGTAGGGG
eRF1 (667/611)	oYZ181		GCCTTAATTAACAAGTTGAATCCCTCGCCG
	oYZ182		GGCCTTAATTAAACAAAGACAGAATGAGCG
Y14 (458/399)	oYZ300		CGACCTCCTGCACTCAACAA
	oYZ301		CCTCAAGCGTCGGATACTCAA

Table S9 Oligonucleotide primers and templates used to generate probes for northern and Southern analyses.

Genes	Template	Fragment (bp)	Oligo	Oligonucleotide sequence, 5′ → 3′
arg-2 (NCU07732)	cDNA*	997	MB001	GTTATAGGAATTCGCGCTTCCACCATGCCCATCTCC
			MB002	CTCTATTCCGCTCGAGTTGTAGCCTTCGGAGGTGAGACC
eif5 (NCU00366)		1278	oYZ405	GCTCTAGATCAATACCGCCAAAATGGG
			oYZ406	GCTTAATTAACTCATCGTCCTCCTCCTCAG
eif4a3 (NCU01234)		1150	oYZ195	GATCTAGACAGAATCGCCCACCATG
			oYZ196	GCTTAATTAAGGAGATAAGGTCGGCAACATTCATGGGC
eRF1 (NCU00410)		757	oYZ121	ACTTCGTCTTCCTCATCTTCTTCAC
			oYZ120	AGGCGTTCAGGTCGTTCTTG
cox-5 (NCU05457)		396	MB005	GTTATAGGAATTCGCGCTTCCACCATGCCCATCTCC
			MB006	CTCTATTCCGCTCGAGTTGTAGCCTTCGGAGGTGAGACC
luc	pRMP57	663	oYZ167	ACATCACCTACGCCGAGTACTTC
			oYZ188	TCCTCCTCGAAGCGGTACA
his-3 (NCU03139)	cDNA*	1761	oYZ069	CCACCGTTGTCGTTGATGAG
			oYZ068	GAGTAATCGCCAACGGACTCA
bar	pBARGPE1	300	oYZ487	CAACCACTACATCCAGACAAGCA
			oYZ486	ACAGCGACCACGCTCTTGA
mago (NCU04405)	cDNA*	602	oYZ377	GCTCTAGAAGCAACAAACAGCCATGTCAGC
			oYZ378	CCTTAATTAAAATGGGCTTGATCTTGAAGTGC
y14 (NCU03226)	cDNA*	519	oYZ375	GCTCTAGAACGTAGAAGCTGCTAAAATG
			oYZ376	CCTTAATTAACTCGTCCCTGCCAACG

*DNase I treated total RNA was used as template to synthesize first-strand cDNA with a combination of oligo$(dT)_{18}$ and random hexamer primers as described in Materials and Methods

Table S10 List of transcripts and oligonucleotide primers used for qPCR.

Genes	Oligo	Position	Oligonucleotide sequence, 5′ → 3′
25S	oYZ029	1794	CCGCGGGAGGGAATAATT
	oYZ030	1849	GGAGACCTGCTGCGGTTATG
luc	oYZ187	787	ACGGCTTCGGCATGTTCA
	oYZ188	865	TCCTCCTCGAAGCGGTACA
upf1 (NCU04242)	MSS169	1284	CAAGCTGCTGGGACACGAA
	MSS170	1347	GTGGAACTTCTTGGGCATCGTA
upf2 (NCU05267)	oYZ055	3514	CCGGGAGAACGATGATTATGA
	oYZ056	3578	GATCGGAGCGGTTATGGTGAT
upf3 (NCU03435)	oYZ061	167	TCGGCGATGAATGGAAAGTC
	oYZ062	227	TTGCCAGGCCAGTATGAAAAC
mago (NCU04405)	oYZ009	260	AATGGCCGACCAAAAACAAA
	oYZ010	314	TTCCCGAGGCGGATCTC
y14 (NCU03226)	oYZ299	429	ACAGGCGAAGCGGTTACG
	oYZ300	485	CCTCAAGCGTCGGATACTCAA
cbp20 (NCU00210)	oYZ379	450	TCARGGARCGCRTCTRCGARTTGRC
	oYZ380	508	TGARTGCRGCTRCGTRCCARACTRT
cbp80 (NCU04187)	oYZ459	470	TGGRTGTRCTTRCCCRCGTRGTTRG
	oYZ460	533	GGARACTRGGCRAGTRCTGRCAARGTC
arg-2 (NCU07732)	MB019	315	CACCCAGCCCTTGATTGG
	MB020	373	GGTTGAACTCGTCACGCTCAT
eif5 (NCU00366)	oYZ251	17	TCAACGTTCGTCGGGACAA
	oYZ252	79	TGGTCTGGATACGCTCCATCT
inl (NCU06666)	oYZ271	1336	CTTGCCTCGCCCCTGAT
	oYZ272	1395	CTGGATGCGGGTCATGATC
eif4a3 (NCU01234)	oYZ023	486	TCATCTCCGCACCAGACACA
	oYZ024	543	GAGGAGCTCATCGGCTTCAT
eRF1 (NCU00410)	oYZ119	727	CGTTGCCGGTCTCGTTTT
	oYZ120	782	AGGCGTTCAGGTCGTTCTTG
xrn1(NCU06678)	oYZ357	1454	AGCRCGTRTCTRCCGRTATRCATRCAA
	oYZ358	1516	TCGRGCCRGCARGTTRAAARTCC
cox-5 (NCU05457)	MSS177	402	GCAAGAGGCTACCAACGAGTTC
	MSS178	469	CTTCGGAGGTGAGACCAGTGA
uc-4 (NCU01446)	MB063	91	GCCGTCAACTTCGACAACGT
	MB064	156	AATGCTGAGGAGAGCGATGAG

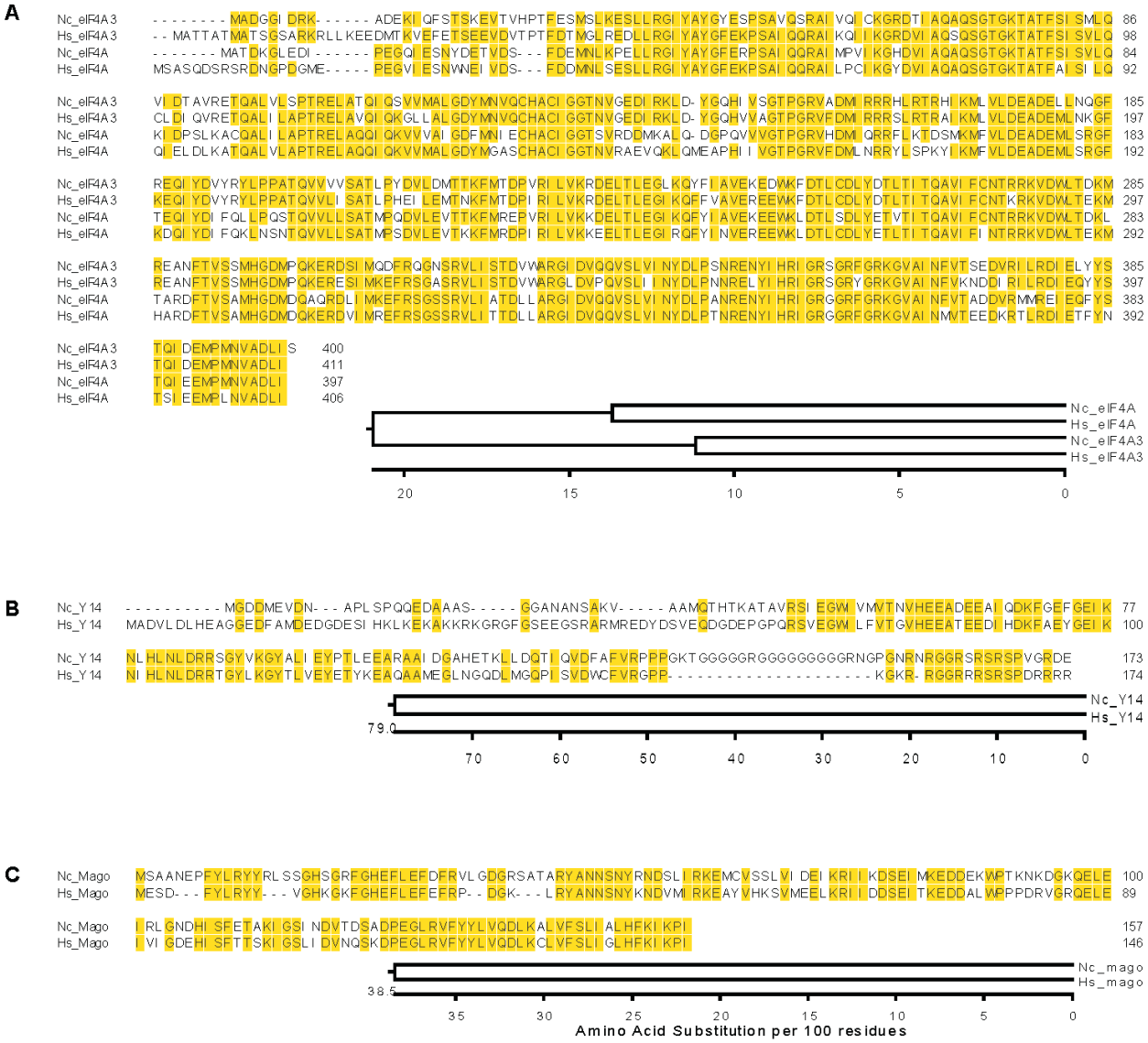

Figure S1 Proteins sequence alignments of eIF4A3, Y14 and Mago.

Protein sequence alignment showing sequence conservation of (A) eIF4A3 and eIF4A, (B) Y14, (C) Mago; alignments and phylogenetic trees were constructed with CLUSTALW using DNASTAR® (version 11.2.1). Completely conserved residues are highlighted in yellow.

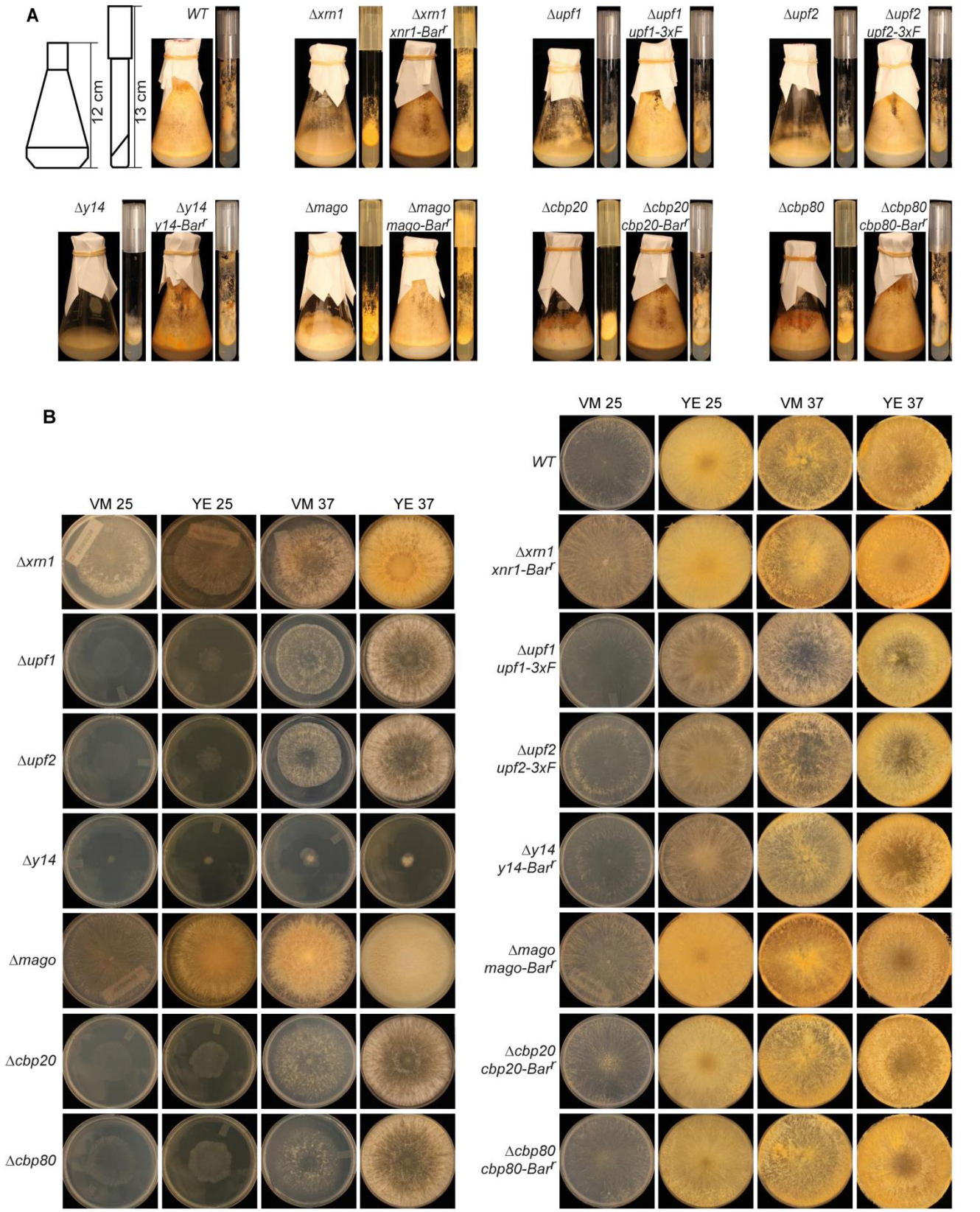
A
12 cm
13 cm
WT
Δxrn1
Δxrn1 xnr1-Barr
Δupf1
Δupf1 upf1-3xF
Δupf2
Δupf2 upf2-3xF
Δy14
Δy14 y14-Barr
Δmago
Δmago mago-Barr
Δcbp20
Δcbp20 cbp20-Barr
Δcbp80
Δcbp80 cbp80-Barr
B
VM 25
YE 25
VM 37
YE 37
Δxrn1
Δupf1
Δupf2
Δy14
Δmago
Δcbp20
Δcbp80
WT
Δxrn1 xnr1-Barr
Δupf1 upf1-3xF
Δupf2 upf2-3xF
Δy14 y14-Barr
Δmago mago-Barr
Δcbp20 cbp20-Barr
Δcbp80 cbp80-Barr

Figure S2 Phenotypes of mutant strains.

(A) *N. crassa* wild type (wt, FGSC2489), and the indicated deletion and corrected-deletion strains Δ*xrn1* (NCU06678 FGSC19228), Δ*xnr1 xrn1*-Bar^r, Δ*upf1* (NCU04242, FGSC11230), Δ*upf1 his-3*::*upf1*-3XFLAG, Δ*upf2* (NCU05267, FGSC15706), Δ*upf2 his-3*::*upf2*-3XFLAG, *Δy14* (NCU03226, FGSC15492), *Δy14 y14*-Bar^r, *Δmago* (NCU04405, FGSC13031), *Δmago mago-Bar^r*, *Δcbp20* (NCU00210, FGSC18692), *Δcbp20 cbp20*-Bar^r , *Δcbp80* (NCU04187, FGSC22440), and *Δcbp80 cbp80*-Bar^r were grown in 1X VM/1.5% sucrose/2% agar at 25°C for 4 days in 125 ml flasks containing 25 ml medium or for 4 days in 16x125 mm culture tubes containing 3 ml medium. (B) The strains shown in panel (A) were grown by inoculating the centers of 100 mm Petri plates containing 1X VM/1.5% sucrose/2% agar with or without 2% yeast extract (YE) and incubating the plates at 25°C or 37°C for 48 hr.

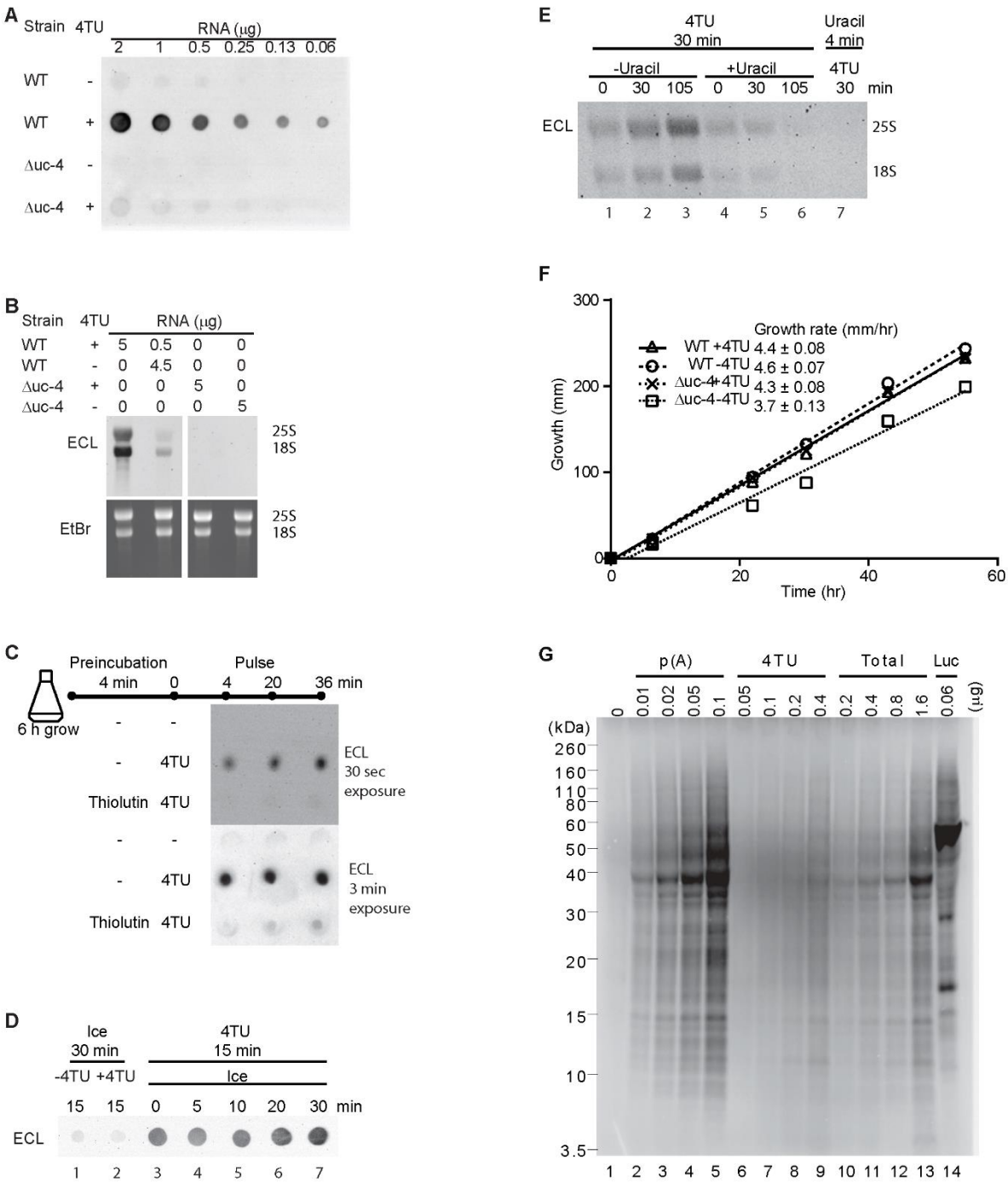

Figure S3 Validation of the 4TU pulse-chase protocol.

(A) ECL detection of biotinylated RNA prepared from wt or *Δuc-4 N. crassa* cultures germinated for 6 hr and incubated for 15 min with 0.2 mM 4TU (+) or without 4TU (-). Total RNA was prepared and biotinylated. The biotinylation probe is designed to react with the thio-group in 4TU-labeled

RNA. Serial dilutions of biotinylated RNA were spotted directly on nylon membrane at the indicated amounts. (B) Biotinylated RNA (5 μg/lane) was subjected to denaturing agarose gel electrophoresis and then transferred to membrane. The presence of biotinylated-4TU RNA was assessed using streptavidin coupled to horseradish peroxidase and incubation with ECL reagent. *25S* and *18S* rRNA bands stained with ethidium bromide are shown below. (C) Thiolutin blocks incorporation of 4TU into RNA. *N. crassa* wt cultures were germinated for 6 hr and treated with thiolutin (0.5 μg/ml) or not treated. Then 0.2 mM 4TU was added to cultures and samples were taken 4, 20 and 36 min following addition of 4TU. Total RNA was prepared and biotinylated; 1 μg of biotinylated RNA was spotted on nylon membrane and biotinylated 4TU RNA detected by ECL. Top panel, 30 sec exposure; bottom panel, 3 min exposure. (D) Chilling of cultures on ice reduces incorporation of 4TU. Lanes 1 and 2: 6 hr germinated wt cultures were placed on ice for 30 min; then 0.2 mM 4TU was added (lane 2) or not added (lane 1) and incubation on ice continued for 15 min; incorporation of 4TU into RNA was examined by dot-blotting and ECL. Lanes 3-7: a 6 hr germinated wt culture was incubated with shaking for 15 min at 30°C with 0.2 mM 4TU; then uracil was added to 10 mM and the culture quick-chilled by mixing with 7 ml VM/2% sucrose/10 mM uracil that had been pre-frozen in a 50 ml conical centrifuge tubes. The chilled culture was placed on ice and cells were harvested by filtration at 0, 5, 10, 20 and 30 min time points. For ECL analyses in lanes 1-7, total RNA was prepared and biotinylated; 1 μg of biotinylated RNA was spotted on nylon membrane and biotinylated 4TU RNA detected by ECL. (E) Lanes 1-6: Cultures of conidia from wt were germinated for 5.5 hr and then were treated with 0.2 mM 4TU for 30 min. Then 10 mM uracil was added to cultures using a 0.25M stock prepared in DMSO (+uracil, lanes 4-6) or the equivalent volume of DMSO was added (- uracil, lanes 1-3). Cells were harvested 0, 30 and 105 min later by filtration. In a separate analysis (lane 7), a 7 hr germinated culture were pretreated with 10 mM uracil for 4 min, then incubated with 0.2 mM 4TU for an additional 30 min, and then harvested by filtration. For lanes 1-7, total RNA was prepared and biotinylated; 2.5 μg of biotinylated RNA was subjected to denaturing agarose gel electrophoresis and then transferred to membrane. The presence of biotinylated-4TU *25S* and *18S* RNA was detected with ECL reagent. (F) Effects of 4TU on growth in race tubes. wt and *Δuc-4* strains were grown in race tubes containing VM/1.5% sucrose/2% agar with or without 0.2mM 4TU at 30°C with 12:12 hr L:D for 60 hr. The growth front was marked twice daily and the growth rate was calculated from triplicate experiments. (G) *In vitro* translation of 4TU RNA. Indicated amounts of *N. crassa* poly(A) RNA (Lanes 2-5), 4TU RNA (Lanes 6-9), total RNA (Lanes 10-13) and *in vitro* transcribed synthetic *luc* mRNA that was capped and polyadenylated (Lane 14) were used as templates for *in vitro* translation in micrococcal nuclease-treated wt *N.crassa* cell extracts (Wu *et al.* 2012). A translation reaction with no added template is shown in Lane 1. [^{35}S]Met-labeled translation products were separated on a 12% NuPAGE Bis-Tris Gel (Invitrogen NP0343) and detected by phosphorimaging.

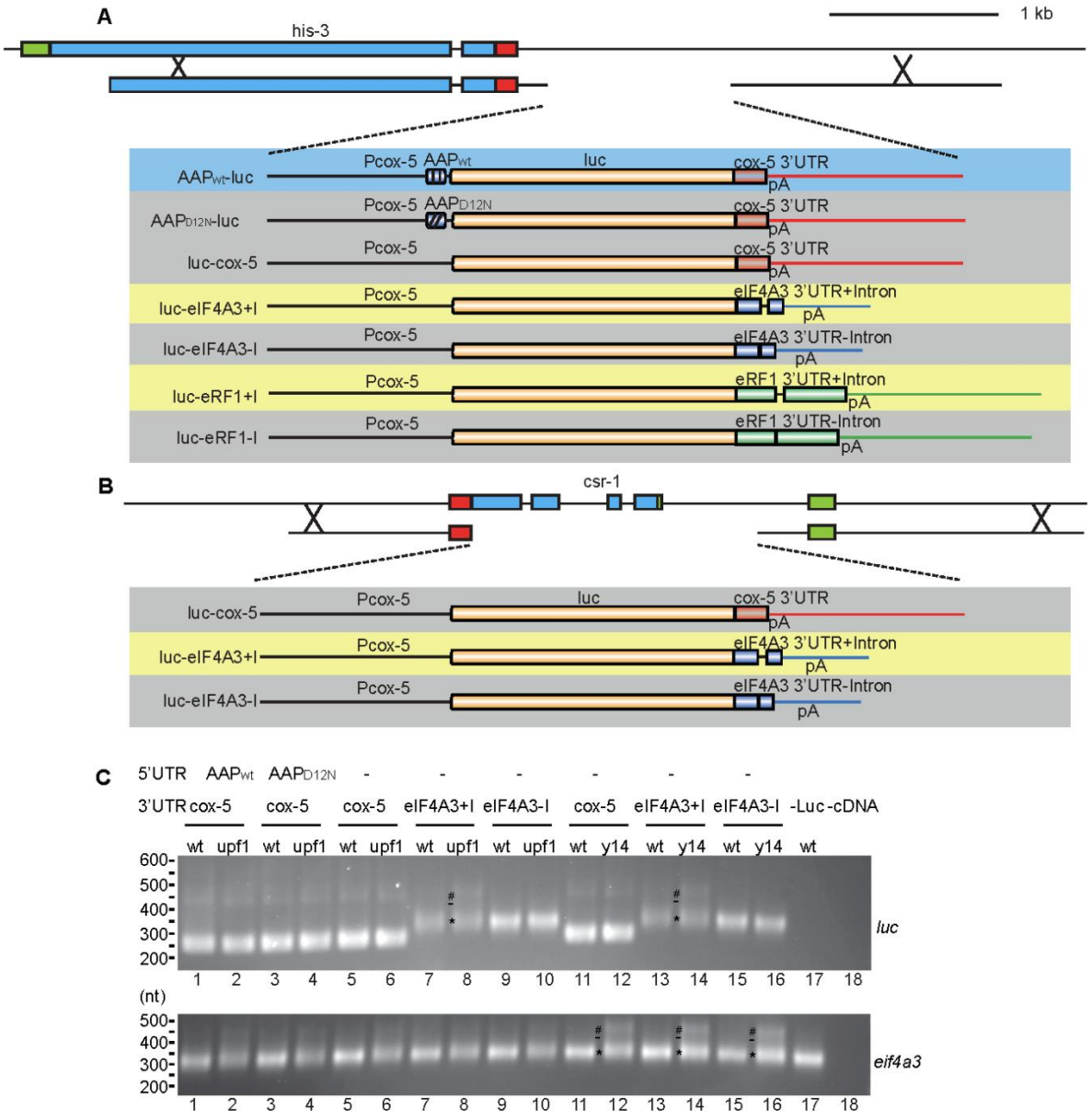

Figure S4 *In vivo* codon-optimized luciferase (*luc*) constructs integrated at *his-3* or *csr-1* for assessing uORF and 3'UTR intron effects on mRNA stability.

Schematic representation of the reporters integrated at (A) *his-3* locus or (B) *csr-1* locus**.** For both recipient loci, boxes indicate mRNA exons; green indicates the 5'UTR, blue indicates coding sequences, and red indicates the 3'UTR. All reporters contained the *cox-5* promoter. Constructs contained the wild-type arginine attenuator peptide (AAP) or the mutated or D12N AAP (AAP_{wt}–luc or AAP_{D12N}–luc) for analyzing the role of the *arg-2*-encoded uORF. To examine the roles of 3'UTR introns, the *cox-5* 3'UTR (luc-cox-5) served as a negative control. The shaded boxes surrounding the constructs indicate the reporter mRNAs contain specific features: blue, uORFs that trigger NMD; yellow, spliced 3'UTRs that trigger NMD; gray, no NMD-triggering features. The functions of 3'UTR introns were examined by comparing intron-containing or intronless *eif4a3* 3'UTRs

(luc-eIF4A3+I or luc-eIF4A-I) or *erf1* 3'UTRs (luc-eRF1+I or luc-eRF1-I). (C) 3'RACE analyses of *luc* and *eif4a3* mRNA 3'UTRs in wt and mutant strains. 3'RACE analysis was performed with specific oligos as described in Materials and Methods. The major and minor bands were excised and sequenced. The major 3'RACE fragment from *luc-cox-5* with oligos oYZ287~oYZ294 was 282 bp (top panel, lanes 1-6, 11,12). The minor larger band was 437 bp and represents an mRNA whose 3'UTR was 155-nt longer. The major fragment from *luc-eif4a3* (spliced-intron or intronless reporters) using oligos oYZ287~oYZ294 was 328 bp (top panel, lanes 7-10, 13-16, position indicated by "*"; the position for unspliced mRNA is 390 bp and indicated by "-"). No fragments were amplified with these *luc*-specific oligo sets from the wt strain lacking a *luc* reporter or from a no-cDNA control (top panel, lanes 17-18). The same cDNAs were used to obtain the endogenous *eif4a3* 3'RACE fragment of 300 bp using oYZ330~oYZ294 (bottom panel, lanes 1~17, position indicated by "*"; the position for unspliced mRNA is 362 bp and indicated by "-"). The larger fragment indicated by "#" observed for *eif4a3* in the *Δy14* strain (387 bp) represents a 3' extension of the spliced mRNA. This 3' extension (415 bp fragment, indicated by "#") is also observed for the spliced-intron *luc-eif4a3* reporter mRNA in the *Δupf1* and *Δy14* strains as determined by sequencing these fragments.

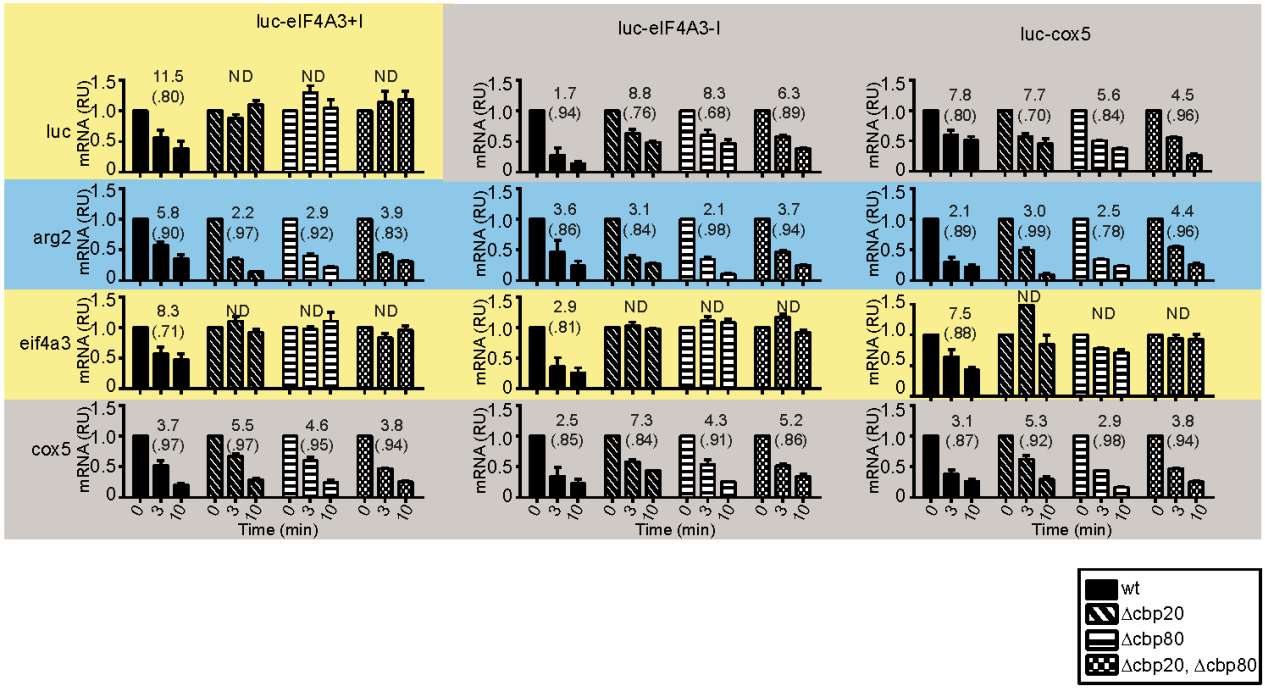

Figure S5 Stability of 3'UTR-intron containing reporters in *Δcbp20*, *Δcbp80* and *Δcbp20 Δcbp80* strains.

Half-lives of mRNA were measured by 4TU RNA pulse-chase (as described in Figure 2) to analyze the effects of three different 3'UTRs on reporter mRNA stability: *eif4a3* 3'UTR intron (left), intronless *eif4a3* 3'UTR (middle); *cox-5* 3'UTR (right), indicated as luc-eIF4A3+I, luc-eIF4A3-I and luc-cox5, respectively. The different reporters were placed in wt, *Δcbp80, Δcbp20* and *Δcbp20Δcbp80* double mutant strains as indicated.

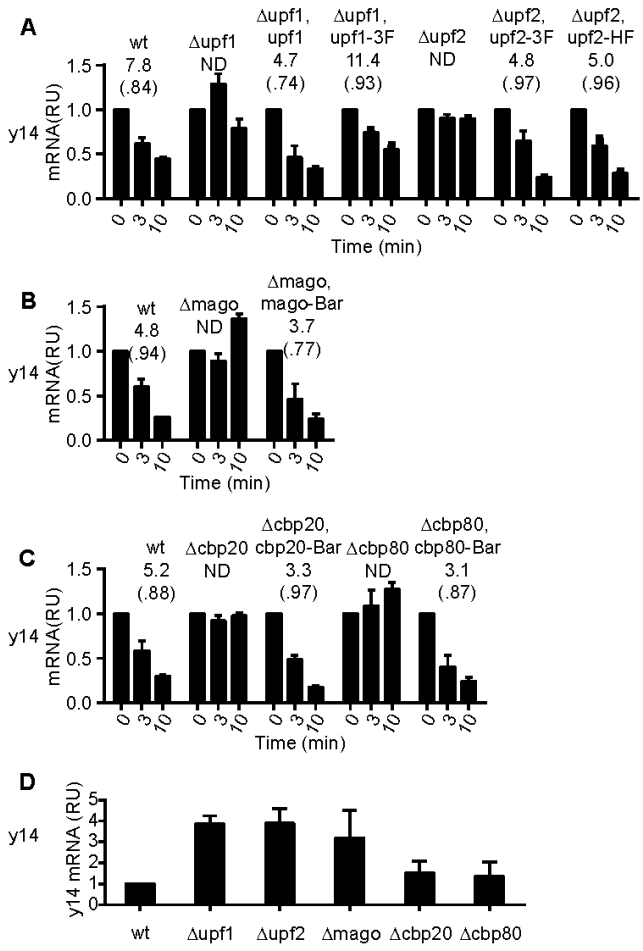

Figure S6 The stability of the spliced 3'UTR intron-containing *y14* mRNA is affected by NMD, EJC and CBC mutations.

(A-C) Half-lives of mRNA were measured by 4TU RNA pulse-chase as described in Figure 2 to analyze the effects of NMD, EJC and CBC mutations on *y14* transcript stability. 4TU RNA was from the same samples used for analyses of other RNAs in other figures (A) wt, Δ*upf1,* Δ*upf1 his-3*::*upf1,* Δ*upf1 his-3*::*upf1*-3XFLAG , Δ*upf2*, Δ*upf2 his-3*::*upf2*-3XFLAG and Δ*upf2*, *his-3*::*upf2*-HAT-FLAG strains (B) wt, *Δmago* and *Δmago mago[Bar^r]* strains (C) wt, *Δcbp20, Δcbp20 cbp20[Bar^r], Δcbp80, Δcbp80 cbp80[Bar^r]* strains. (D) Measurement of mRNA levels of *y14*, *eif4a3*, e*rf1*, *arg-2*, *eif5* and *cox-5* in total RNA in wt, Δ*upf1,* Δ*upf2*, *Δy14, Δmago,Δcbp20* and *Δcbp80* strains. The data for total RNA levels show the average and standard deviations from four independent RNA preparations (mRNA levels were normalized to 25S rRNA levels in each case and all then all calculated relative to the normalized level in wt).

File S1

Supplemental movie

Comparisons of asexual growth and development of wt vs *Δupf1* vs *Δupf1 upf1-3XFLAG:* wt vs *Δupf2,* vs *Δupf2 upf2-3xFLAG;* wt vs*Δy14* vs *Δy14 y14-Bar^r;* wt vs *Δmago* vs *Δmago mago-Bar^r* ;wt vs *Δcbp80* vs *Δcbp80 cbp80-Bar^r;* wt vs *Δcbp20* vs *Δcbp20 cbp20-Bar^r*

10^5 conidia in 5 μl sterile water obtained from the indicated strains were inoculated on a sterile Whatman 451 filter disk placed in the center of a VM/1.5% sucrose/2% agar plate and incubated at room temperature with constant light. Images of growing cultures were taken every 3 min or 5 min for a given experiment, and images collected over an approximately 70-h period of time. Time lapse movies were created at 30 images/sec.

Available for download as an mp4 file at www.genetics.org/lookup/suppl/doi:10.1534/genetics.115.176743/-/DC1